UNIVERSITY OF CALIFORNIA, SAN DIEGO

Senataxin, a modulator of disease pathogenesis in Amyotrophic Lateral Sclerosis

A Thesis submitted in partial satisfaction
of the requirements for the degree Master of Science

in

Biology

by

Matthew Brian Mitchell

Committee in charge:

Professor Albert La Spada, Chair
Professor Lorraine Pillus, Co-Chair
Professor Susan Ackerman

2017

The Thesis of Matthew Brian Mitchell is approved, and it is acceptable in quality and form for publication on microfilm and electronically:

_____

_____
Co-Chair

_____
Chair

University of California, San Diego

2017

DEDICATION

I dedicate this thesis to my family for supporting me through everything. Thank you for always being there for me. I love you all.

TABLE OF CONTENTS

LIST OF FIGURES

ACKNOWLEDGEMENTS

Firstly, I would like to acknowledge Professor Albert R. La Spada for the opportunity he has given me to be a member of his lab and participate in some incredible research. Professor La Spada, as well as all of the post-docs, graduate students and lab members have made my time in the lab a truly unforgettable and life changing experience.

Next, I would like to express gratitude towards Lorraine Pillus and Susan Ackerman for being on my thesis committee. Thank you for your time and support.

Finally, I would like to thank Somasish Ghosh Dastidar for all of his effort and support over these last 3+ years. Thank you for teaching me everything I know about research and always believing in me. If it wasn't for your guidance, I doubt I would be in this position today. Best of luck in the future.

ABSTRACT OF THE THESIS

Senataxin, a modulator of disease pathogenesis in Amyotrophic Lateral Sclerosis

by

Matthew Brian Mitchell

Master of Science in Biology

University of California, San Diego, 2017

Professor Albert La Spada, Chair

Professor Lorraine Pillus, Co-Chair

Amyotrophic Lateral Sclerosis 4 (ALS4) is a rare, early onset, autosomal dominant form of ALS, a neurodegenerative disorder characterized by the progressive loss of motor neurons in the brain and spinal cord. Dominant, gain-of-function mutations in the RNA-binding protein, senataxin (SETX) cause ALS4, but the mechanistic basis for SETX motor

neuron toxicity is unknown. In order to study this phenomenon, an ALS4 mouse model was generated carrying the SETX gene mutation, L389S. These mice exhibit neuromuscular phenotypes and motor neuron degeneration. Primary neurons prepared from these ALS4 mice show signs of neurotoxicity and immunostaining analysis of motor neurons has uncovered nuclear membrane abnormalities. Additionally, a hexanucleotide repeat expansion (HRE) in the gene C9orf72 has been identified as the most common genetic cause of ALS. Separate studies have identified that SETX contributes to C9orf72-ALS disease penetrance and as well acts as a genetic modifier of C9orf72 induced toxicity. Using cells lines and primary neurons we have found that reduced expression of SETX exacerbates C9orf72 HRE dipeptide repeat (DPR) toxicity. Additionally, through density-based fractionation studies we have established the localization of senataxin in the nucleolus and that senataxin forms an interaction with toxic C9orf72 dipeptide repeat proteins.

INTRODUCTION

Amyotrophic Lateral Sclerosis

Amyotrophic Lateral Sclerosis (ALS) is a neurodegenerative disorder characterized as the progressive loss of both upper and lower motor neurons of the brain and spinal cord. Symptoms often include muscle wasting, weakness, and spasticity which originate in the limbs but inevitably progress towards total paralysis[1]. As a classically defined motor neuron disease, ALS is clinically recognized as the scarring and degeneration of the corticospinal motor neurons as well as the deterioration of the lower neurons of the spinal cord. These neurons are responsible for the contractile function of skeletal muscles, and thus their demise subsequently leads to severe muscle degeneration[2]. While not true of all forms of ALS, loss of bulbar function is also commonly experienced, a major factor leading to respiratory failure and ultimately resulting in death. ALS has been documented as both familial (fALS), 10% of known cases, and Sporadic (sALS), 90% of known cases, and although some familial forms of ALS lead to early onset, ALS is primarily known as a disease of the aged with patients succumbing to their symptoms 3-5 years post onset[1,2].

In addition to the loss of motor neurons, ALS pathology is primarily denoted as the formation of inclusions, or protein aggregates which form in both the brain and spinal cord**.** The most notable pathological feature is the formation of cytoplasmic inclusions positive for ubiquitin and the RNA-binding protein, TDP-43, which its aggregation and clearance from the nucleus called TDP-43 proteinopathy, is now considered as a hallmark of the disease. Similarly, prominent ALS genes such as C9orf72, SOD1 (a Cu-Zn superoxide dismutase), and FUS (an RNA-binding protein) have also shown evidence of inclusions[2,3]. But, despite these findings which form a correlation between protein aggregation and ALS, little is known about the role of these aggregates, if any, in disease progression[2].

Since the discovery of SOD1 in 2003, the first ALS gene identified, an upward of 50+ genes have been reported, which include mechanisms in altered proteostasis, disruption of axonal transport and defective RNA metabolism, defined as the synthesis, processing, and degradation of RNA. Despite substantial progress in identifying the primary causative mechanism, mutations in genes such as TDP-43, SOD1 and FUS account for only a small percentage of affected ALS patients[2]. Recently, this changed due to the discovery of a new gene in 2011. The identification of a (G_4C_2) hexanucleotide repeat expansion (HRE) in the gene C9orf72 has led to what is now known as the primary cause of both sporadic and familial forms of ALS. Located on chromosome 9p, the expansion mutation is positioned between Exon 1a and 1b in the first intronic region of C9orf72[4]. Some studies have shown that ~10% of sALS and between 25-40% fALS patients possess this mutation[5]. While repeats in control patients have shown to exist in as little as 2-23 repeats, affected patients can have repeats ranging from several hundred to greater than one thousand[6].

Mechanisms of C9orf72 hexanucleotide repeat expansion

In an attempt to elucidate the molecular basis of C9orf72-ALS, three potential mechanisms have emerged, in which both loss-of-function and gain-of-function have been proposed[7]. Despite evidence which suggests the repeat expansion limits gene expression, very little is known about the effects of haplo-insufficiency. In fact, C9orf72 primarily remains a mystery and a consensus has not been reached about its intended function. For these reasons loss-of-function has not been considered a primary mechanism. Thus, the focus of C9orf72 research has been on two gain-of-function mechanisms 1) the formation of toxic RNA foci and 2) the production of repeat associated non-ATG (RAN) translated

dipeptide proteins[2]. The HRE has been shown to produce RNA foci which accumulate in the brain and spinal cord. Through bi-directional transcription of this gene, it produces both a sense GGGGCC and an anti-sense CCCCGG transcript capable of sequestering RNA-binding proteins through their expanded repeat sequences[2]. The formation of primarily nuclear RNA foci has shown to result in the sequestering of hnRNPs (heterogeneous nuclear ribonucleoproteins) involved in splicing, RNA export proteins and some proteins associated with nucleolar function such as nucleolin, a protein involved in rRNA production and ribosomal assembly. In addition to this, these expanded repeat sequences have been shown to form stable secondary RNA structures called G-quadraplexes through which they are thought to interact with RNA-binding proteins and disrupt RNA metabolism[7,8]. The second gain-of-function mechanism results from the RAN translation of the HRE. First identified in the trinucleotide diseases Spinocerebellar Ataxia 8 (SCA8) and Myotonic Dystrophy-type 1 (DM1), RAN translation has been identified as a reoccurring mechanism in neurodegeneration and amongst microsatellite expansion disorders[9]. This recently discovered mechanism has been characterized as ATG-independent, irrespective of an ATG initiated ORF, repeat-length dependent, and results in the translation of all reading frames without the occurrence of a frameshift. It has also been determined that many of these transcripts are expressed as hairpin loops suggesting the formation of these secondary structures as a requirement for initiation of RAN translation at the ribosome[10]. Translation of the HRE gives rise to 5 unique polypeptide repeat sequences from both the sense and antisense strands. From the sense strand, poly-GA (Glycine-Alanine), poly-GR (Glycine-Arginine) poly-GP (Glycine-Proline), and anti-

sense strand, poly-PR (Proline-Arginine), poly-PA (Proline-Alanine), and poly GP (Glycine-Proline)[8]

C9orf72-ALS pathology is known for its distinctive star shaped inclusions which are primarily localized to the cytoplasm, although some reports suggest nuclear as well as nucleolar localization. They are negative for TDP-43, but positive for ubiquitin, each of the 5 dipeptide repeat proteins (DPRs), and the protein p62 (SQSTM1)[11]. These inclusions have been identified in the cortex, cerebellum, hippocampus, and spinal cord of human tissue[12]. Of the five DPRs, only the highly polar and charged polymers, GR and PR, have consistently shown to be toxic, with nominal evidence to support GA toxicity[11]. In drosophila models, expression of GR or PR give rise to a degenerative eye phenotypes in contrast to the less toxic GA, PA and GP[13,14]. Upon introduction to cell lines (HEK293, NSC-34 and U2OS) and IPSC-derived neurons, GR and PR accumulate in the nucleus, induce cell death and drive disease progression[15-17].

C9orf72 GR and PR dipeptide induced toxicity is thought to arise from alterations to splicing and disruption of membrane-less organelles[18,19]. GR and PR contain highly repetitive arginine rich sequences which are reminiscent of the highly conserved mRNA splicing factors, SR proteins. These splicing factors often interact with RNA-binding proteins (RBPs), through an evolutionarily conserved sequence called low complexity domains (LCD)[18]. These sequences allow for transient and low affinity interactions necessary for the liquid-like assembly and proper function of membrane-less organelles. Such as, but not limited to, the nuclear pore complex and sites of RNA processing such as nuclear speckles, cajal bodies, stress granules, and nucleoli. Interestingly, the GR and PR interactome is largely composed of proteins which contain LCDs, making up ~2/3 of GR

and PR common interactors[13,18,19]. RBPs localized to nuclear speckles (regions enriched with pre-mRNA splicing factors) and cajal bodies (the sites of spliceosome assembly) have been identified as genetic modifiers as well as GR and PR specific protein interactors[18]. Disruption of these membrane-less organelles is evidenced by missplicing events which occur as a result of GR and PR expression. *In vitro,* PR has shown to associate with RBPs and induce alterations to global pre-mRNA splicing including exon skipping, introduction of alternative UTRs, and inclusion of introns[17]. A recent study has revealed a probable mechanism in which U2 small nuclear ribonucleoprotein particles (snRNP), which function in splicing and possess LCDs, directly bind GR and PR. This interaction has been shown to impede spliceosome formation and cause mislocalization of snRNPs from nuclear speckles to the cytoplasm[20].

GR and PR also exhibit a strong nucleolar localization, in which they alter the expression and maturation of rRNA. Through binding of nucleoli, GR and PR alter production and processing of 18s, 5.8s and 28s rRNA necessary for ribosomal biogenesis[17]. Accumulation of GR and PR in the nucleolus has also shown evidence of nucleolar swelling, translocation of B23 from the nucleolus as well as dispersion of Nucleolin[15,16]. Additional studies have revealed that PR localizes to the granular component of the nucleolus while GR can localize to both the granular component and fibrillary core, both forming direct interactions with nucleolar proteins involved in regulation of rRNA expression and processing[18].

Most notably, prominent ALS genes, TDP-43, FUS, ATXN2, and hnRNPA1 which appear in membrane-less organelles such as nuclear speckles and stress granules, have been identified in the GR and PR interactome as well as genetic modifiers of DPR toxicity.

Interestingly, many disease causing mutations in these RBPs reside in the LCD, suggesting alterations to the dynamics of membrane-less organelles which function in RNA processing, as a point of interest[18]. Genes such as TDP-43, play an essential role in regulating RNA processing pathways, in which loss-of-function has shown to cause global alterations to splicing and gene expression[21]. Additionally, new evidence suggests that TDP-43 functions in repressing non-conserved cryptic exons, which are thought to contribute to cell death and TDP-43 proteinopathy[22]. This commonality between C9orf72-ALS and less common forms of both sporadic and familial ALS suggests shared molecular pathways and pathogenic features which results from impaired RNA metabolism.

Senataxin (SETX)

Amyotrophic Lateral Sclerosis 4 (ALS4) is a non-lethal, rare, early-onset familial form of ALS. Patients suffer from an array of symptoms, including, but not limited to atrophy of muscles of the lower limbs and hands, proximal muscle weakness, and eventual wheel-chair dependence, requiring lifelong care and medical assistance. In addition to this, symptoms are described as slowly progressing and absent of sensory neuron and bulbar involvement. ALS4 is known to exclusively result from several dominantly inherited point mutations in the gene SETX[23]. Senataxin (SETX) is a large RNA-binding protein, absent of a low complexity domain (LCD), with a highly conserved DNA/RNA helicase domain which functions in the resolution of R-loops or DNA/RNA hybrids which form between template DNA and nascent RNA strands. In addition to these functions, SETX serves various roles in RNA metabolism which include regulation of transcription termination, RNA processing and mediating functions of the nuclear exosome. (CL Bennett and SG Dastidar – manuscript submitted). As well, Senataxin has considerable homology to two

human helicase genes, RENT1 and IGHMBP2, both of which have functions implicated in RNA metabolism and cell survival[24]. Interestingly, senataxin joins a list of genes involved in RNA metabolism which are known to cause familial forms of ALS, some of which include TDP-43, SMN, and FUS[23]. Following its discovery in 2004, research efforts have led to the identification of several notable gain-of-function mutations: T3I, R2136H, and L389S located in both the N-terminal protein-interaction domain (T3I, L389S) and the enzymatic helicase domain (R2136H), all of which are known to cause ALS4[24]. Alternatively, loss-of-function mutations in SETX do not result in ALS4, but have been identified to cause another related neurodegenerative disorder, Ataxia with Oculomotor Apraxia 2 (AOA2). Not unlike ASL4, this disease is characterized as early onset and slow progressing but in contrast results in cerebellar degeneration and loss of oculomotor function[25].

Sen1p, the yeast orthologue of SETX, possesses a highly conserved helicase domain and has been implicated in roles of transcriptional regulation and RNA processing[26,27]. This is evidenced by interactions with, Rnt1p, an endonuclease involved in RNA maturation, and Rpo21, a subunit of RNAPII. In addition to these functions, Sen1p has shown to regulate processing of tRNA, rRNA, snRNA, and snoRNA[26]. Interestingly, interactome studies suggest that senataxin retains several of these functions, through interaction with several hnRNPs (heterogeneous nuclear ribonucleoproteins) involved in RNA processing, RNAPII and poly (A)-binding protein, components of transcriptional machinery and the gene, survival motor neuron (SMN), a gene associated with small nuclear RNAs (snRNA). In fact, reduced expression of SETX has been shown to exhibit altered splicing efficiency and inclusion of alternative splice sites[26]. Furthermore, Sen1p

has been shown to engage in essential processes in the nucleolus, including processing of rRNA precursors and snoRNAs, thereby maintaining the integrity of the nucleolus[23]. Some studies have suggested that senataxin maintains nucleolar function, as evidenced by interaction with nucleolar protein, nucleolin, a gene associated with regulation of pre-rRNA transcription and ribosome assembly[26]. As well, this is supported by evidence that senataxin has also been shown to co-localize with fibrillarin, a nucleolar marker which is expressed in the fibrillar center of the nucleolus. Despite this, the majority of published findings suggest a primarily nuclear function with little known, if any, about the role of senataxin in the nucleolus[28].

A known interactor of RNAPII and PABP, senataxin has been shown to regulate the process of transcription termination[27,29]. The release of RNAPII from the template is dependent on both the presence of a poly (A) signal sequence and a downstream terminator sequence. Of the two known terminator sequences, G-rich transcriptional pause sites slow down RNAPII elongation and subsequently result in cleavage of the polyadenylation site and degradation mediated by the 3'-5' exonuclease, Xrn-2. Senataxin, regulates this process through resolution of DNA/RNA hybrids, R-loops, which form over pause sites and recruits Xrn-2 to promote transcription termination[27]. In fact, some studies have shown that depletion of SETX, through use of RNAi, results in differential RNAPII binding and abnormal termination, in which transcription proceeds beyond the terminator sequence[26]. Furthermore, this function of senataxin as a master regulator of transcription termination is reminiscent of Sen1p which functions in regulating expression of many coding and non-coding RNA.

Senataxin has been shown to interact with the exosome, a highly regulated 3'-5' exonuclease[30]. This, primarily nuclear as well as nucleolar, protein complex has been associated with functions which include RNA maturation and processing, RNA turnover, and surveillance of aberrant RNA transcripts[31]. This interaction with both EXOSC9, core component of the exosome and EXOC10, the enzymatic component of the nuclear exosome, has been found to be dependent on the post-translational modification of SUMOylation (small ubiquitin-like modifiers)[30,32]. Mutations in SETX which cause AOA2, but not ALS4, have been found to inhibit both SUMOylation and subsequent interaction with the exosome. To further this point, the exosome and SETX have been found to co-localize in the presence of transcription-related DNA damage. This is believed to be in response to collisions between the replisome and transcription machinery, and suggests a role for SETX in coordinating the function of the exosome[30].

SETX is a modulator of ALS4 and C9orf72-ALS

In an independent study to identify high risk sALS and fALS genes, senataxin, along with TDP-43 and FUS, were determined to be one of the most prominent disease variants in a population of 444 ALS patients. Occurring at a frequency of 2.48% and making up 19.4% of all documented genetic variants[33]. Interestingly, separate independent studies have identified senataxin variants in patients who were also positive for TDP-43 and C9orf72 mutations[34]. Begging the question, could SETX play a role as a contributor to C9orf72-ALS disease penetrance?

Our lab first observed the genetic connection between senataxin and C9orf72 in two transgenic *drosophila* C9orf72-ALS disease models – 1) RAN translated $(G4C2)_{58}$-GFP and 2) ATG-dependent synthetic, non G4C2, GFP-GR_{50}. The phenotype observed in

the $(G4C2)_{58}$-GFP transgenic model included muscle, eye, and neuromuscular junction degeneration. In addition to this, immunofluorescence revealed the formation of RNA foci and the presence of RAN translated dipeptides, as previously reported in various C9orf72 models. In an effort to identify modifiers of C9orf72 toxicity observed in fly models, a genetic screen was performed revealing a list of potential enhancers and suppressors. The genetic modifiers identified included components of the nuclear pore complex, nuclear export/import proteins, components of the nuclear exosome, and the DNA/RNA helicase, Senataxin[13].

This astonishing revelation was further confirmed by the generation of SETX-WT and SETX-L389S transgenic *drosophila* using GAL4/UAS system. Expression of SETX-WT and SETX-L389S exhibited a complete rescue of the aforementioned degeneration attributed to both GFP-GR_{50} and $(G4C2)_{58}$-GFP C9orf72 transgenic models, resulting in 100% viability.

Here, using an *in vitro* cell line and primary neuron model, we show that senataxin acts as both a genetic modifier and an interactor of C9orf72 DPRs. In an effort to recapitulate *drosophila* studies which suggest senataxin is a potent suppressor of GR induced toxicity, we have observed that reduced expression of senataxin can exacerbate GR toxicity and that senataxin exhibits preferential binding of GR, without the presence of a low complexity domain. In addition to these findings, we show that senataxin exhibits a prominent nucleolar localization and RNA-mediated interactions, suggesting potential mechanisms for these findings.

Furthermore, to determine the molecular basis of SETX gain-of-function mutations which cause ALS4, our lab has generated two ALS4 mouse models. 1) SETX L389S, “knock in”

model and 2) SETX R2136H, transgenic model, using mouse prion protein promoter (PrP). Both PrP-SETX-R2136H and SETX-L389S$^{+/-}$ mice have been characterized as having a slowly progressive motor phenotype, motor neuron dysfunction and the hallmark characteristic of TDP-43 mislocalization. Using immunostaining of spinal cord sections, we have found that SETX-L389S$^{+/-}$ primary neurons display defects in nuclear membrane morphology. Additionally, in an effort to evaluate the effects of SETX L389S, we have also shown that primary neurons carrying SETX mutations exhibit neurotoxicity and are driven towards cell death. These finding aim to emphasize the importance of senataxin in neuron survival and establish a common link between ALS4 and C9orf72- ALS disease mechanisms.

RESULTS

SETX L389S primary neurons exhibit increased susceptibility to cell death

To evaluate SETX L389S$^{+/-}$ neurotoxicity, primary cortical and cerebellar granule neurons from SETX L389S$^{+/-}$ mice were dissociated and grown in culture. Cerebellar granule neurons (CGN) are profoundly sensitive to potassium levels and have a tendency to undergo apoptosis if exposed to a medium containing low, non-depolarizing, concentrations of potassium (LK)[37,38]**.** Control and SETX L389S$^{+/-}$ CGNs were cultured in medium containing high concentrations of potassium (HK) and then replaced with LK medium for 8 and 20 hours and stained with propidium iodide (PI), a red-fluorescent, membrane impermeable cell viability stain (Figure 1A). SETX L389S$^{+/-}$ CGN were shown to have an increased number of PI positive cells, an indicator of cell death (Figure 1B). Increased levels of cell death was also confirmed using lactate dehydrogenase (LDH) colorimetric cytotoxicity assay, in which SETX L389S$^{+/-}$ CGN were shown to have an increased level of LDH release (Figure 1C). These findings were confirmed by culturing CGN in LK conditions for 6 and 8 hours, western blot analysis shows an increased levels of cell death, as indicated by induction of cleaved caspase 3, in SETX L389S$^{+/-}$ CGN as compared to control littermates (Figure 1D-1E). Additionally, primary cortical neurons (PCN) were also dissociated from SETX L389S$^{+/-}$ cortex and grown in culture. After 14 days in normal, unstressed, growth conditions, PCN exhibited a significantly high level of cytotoxicity as shown by a marked increase PI positive cells (Figure 2A-2B).

SETX L389S motor neurons display defects to nuclear membrane morphology

Defects of nucleocytoplasmic transport and the nuclear membrane are a shared feature of more common forms of ALS such as C9orf72-ALS[13]. Because of this, alterations to the nuclear membrane in SETX L389S$^{+/-}$ was investigated. Using L5 lumbar spinal cord

sections, motor neurons of the ventral horn were subjected to immunostaining for nucleocytoplasmic transport factors, Ran and RanGAP1, which clearly outlined the structure of the nuclear membrane. Analysis of immunostaining revealed that SETX L389S$^{+/-}$ showed signs of nuclear invaginations and changes to the overall morphology of the nuclear membrane as compared to the control littermates (Figure 3A-3B). These alterations to the nuclear membrane were quantified for both Ran and RanGAP1, and SETX L389S$^{+/-}$ demonstrated a fold increase in motor neurons positive for this abnormality (Figure 3C).

Reduced expression of SETX induces cell death in primary cortical neurons

In order to evaluate the neurotoxic effects of non-physiological levels of senataxin in primary neurons, a SETX shRNA was generated and packaged into a lentiviral transfer vector. PCN were transduced with SETX shRNA or non-target shRNA and harvested 7 days later for analysis. Cells transduced with SETX shRNA demonstrated a ~50% knockdown of senataxin at the transcript levels using qPCR (Figure 4D). To further assess the efficiency of the knockdown, western analysis was performed and found a comparable reduction of expression at the protein level (Figure 4A-4B). Despite only a modest reduction of senataxin expression, this still proved to induce a significant level of toxicity in primary neurons (Figure 4C).

C9orf72 poly-GR, but not poly-GA, induces toxicity in primary cortical neurons

C9orf72 hexanucleotide dipeptide repeat (DPR) constructs were acquired from Dr. Zheng Ying, Soochow University College of Pharmaceutical Sciences. DPR constructs for pEGFP control, pEGFP-GA$_{30}$ pEGFP-GR$_{30}$ were packaged into lentivirus and generated to

determine toxicity in a primary neuron model. Upon transduction of C57Bl6/j primary cortical neurons with DPRs, GR_{30} displayed a primarily nuclear and nucleolar localization with a diffuse cytoplasmic signal, while GA_{30} expression was evenly dispersed. Cytotoxicity was measured 7 days post transduction using LDH and PI staining (Figure 5A). As anticipated, overexpression of GR_{30} but not GA_{30} was sufficient to cause cell death (Figure 5B-5C).

Toxicity induced by various C9orf72 models is exacerbated by reduced expression of SETX

To corroborate previous studies which indicates a link between SETX and C9orf72 in *Drosophila melanogaster,* a C9orf72 mouse model (C9-450B) was utilized. These mice were generated by Dr. Don Cleveland, Department of Cellular and Molecular Medicine, University of California, San Diego. C9-450B contain a Bacterial Artificial Chromosome (BAC) expressing human C9orf72 ALS patient transgene with a $(G_4C_2)_{450}$ repeat and have been documented as having C9orf72 associated RNA foci and DPR inclusions, as well as some behavioral and cognitive abnormalities[35]**.** In untreated conditions, C9-450B PCNs showed induction of cleaved caspase 3 as compared to control littermates (figure 6A-6B). PCN from C9-450B mice were also transduced with SETX and non-target shRNA, and cells were then harvested 7 days post transduction for LDH. SETX shRNA was able to exacerbate toxicity induced by C9-450B, showing greater LDH release relative to control littermates transduced with non-target shRNA (Figure 6C). To support these findings, HEK293T cells were transfected with GA_{30} and GR_{30} with control or SETX siRNA. 48 hours post transfection, cells were evaluated for cell death using propidium iodide. As

expected from previous studies[15], cells transfected with GR_{30} showed relatively high levels of PI positive cells when compared to GA_{30}. Additionally, GR_{30} transfected cells showed increased cytotoxicity upon co-expression of SETX siRNA (Figure 6D). Furthermore, C57Bl6/j PCNs were co-transduced with EGFP-GA_{30}, EGFP-GR_{30}, EGFP control and either non-target shRNA control or SETX shRNA. 7 days post transduction, cell death was assessed using PI staining and LDH and showed increased toxicity in cells co-expressing GR_{30} and SETX shRNA. (Figure 6E-6F). These results suggest that reduced expression of SETX can exacerbate GR toxicity. Unfortunately, the inverse of this study, overexpression and rescue, was not possible. This was due to the large molecular weight of SETX, which exceeded the size limitations for packaging into a lentiviral transfer vector.

Senataxin localizes to the nucleolus and displays a preferential interaction with C9orf72 poly-GR

To determine the localization of endogenous senataxin, subcellular density-based fractionation was used to isolate cytoplasmic, nuclear membrane, nucleoplasmic, and nucleolar fractions from five 15-cm^2 dishes of HEK293T cells. A series of sucrose gradient centrifugation steps were used to fractionate each of the four subcellular fractions (Figure 7A). Western blot analysis reveals that endogenous senataxin displays a prominent nucleolar localization, and comparatively low expression in the cytoplasm, nuclear membrane, and nucleoplasm. Additionally, interactors of Senataxin, EXOSC9, the core exosome, was shown to have a prominent nucleolar signal, as well, EXOSC10, a component of the nuclear exosome, was shown to be almost exclusively nucleolar (Figure 7B).

Previous findings have shown that many RNA-binding proteins that act as genetic modifiers of GR can also display a protein interaction with GR and PR[18]. In fact, upon transfection of HEK293T cells with pEGFP-GA_{30} and pEGFP-GR_{30} plasmid constructs, GR displays a prominent nucleolar localization, which supports the possibility of a senataxin and GR interaction (Figure 8A). Given this, co-immunoprecipitation was used to evaluate this possibility. To test this, HEK293T cells were co-transfected with Flag-SETX and all five GFP-tagged DPR proteins and a GFP control, lysates were then harvested and underwent immunoprecipitation. Western blot analysis reveals a distinct interaction between GFP-tagged GR_{30} and Flag-SETX. Additionally, Senataxin also displays an interaction with GFP-tagged PR_{30}, but no other DPR proteins. This interaction with GR_{30} appears much more significant, thus suggesting a preferential binding of GR (Figure 8B).

Senataxin exhibits RNA-mediated interactions with poly-GR and exosome

The interactome of RNA processing proteins, such as TDP-43, is deeply influenced by the presence of RNA and form many RNA-mediated protein interactions[39]. Given this finding, a similar mechanism was investigated for the observed GR and senataxin interaction. To define this interaction as RNA-dependent, co-immunoprecipitation was performed in the presence and absence of RNaseA. Treatment with RNaseA has been verified as a viable method for identifying RNA-dependent protein interactions, in which TDP-43 and hnRNPH do not Co-IP in the presence of RNaseA[39]. To test this, HEK293T cells were transfected with either Flag-SETX and EGFP-GR_{30} or Flag-hnRNPH, positive control, for 48 hours. Lysates were then harvested, treated with RNaseA, and subjected to immunoprecipitation. Western blot analysis shows a marked reduction in senataxin-GR

interaction in RNaseA treated lysates (Figure 9A). Although this interaction was not completed ablated upon treatment with RNAseA, it suggests a significant degree of RNA dependence. Additionally, the exosome, which functions in RNA processing and degradation, has also been shown to display coordinated function and interaction with senataxin[30]. Using a similar methodology, western blot analysis determined a significantly diminished interaction between senataxin and exosome upon RNaseA treatment, suggesting an interaction which is almost entirely dependent on an RNA intermediate (Figure 9B-9C).

DISCUSSION

In recent years, considerable efforts have been made to elucidate the cellular and molecular mechanisms which give rise to ALS and drive disease progression. Through intensive investigation, several disease mechanisms have emerged to which a substantial amount of evidence has implicated alterations in RNA metabolism as a major factor which can disrupt key homeostatic processes and influence cell survival. The production of abnormal coding and non-coding RNA as well as defects in RNA-binding proteins which mediate RNA transcription, processing and degradation, have been established as a reoccurring theme in ALS biology[2].

Senataxin (SETX), an RNA-binding protein with a highly conserved DNA/RNA helicase domain and the cause of the rare motor neuron disease ALS4, has been associated with many functions which include transcription termination, RNA processing, and mediating functions of the nuclear exosome. To better understand how senataxin results in ALS4, our lab has generated two ALS4 mouse models which exhibit motor neuron dysfunction and the hallmark ALS trait of TDP-43 mislocalization. Although the mechanism has yet to be determined, it is believed that senataxin's role in regulating key RNA processing pathways is an essential component in the mechanistic basis of ALS4. In fact, this theme of RNA metabolism is only further supported by new evidence in which our lab has established a connection between senataxin and the much more common C9orf72-ALS, which results in toxic RNA foci and repeat associated non-ATG (RAN) translated dipeptide repeat (DPRs) proteins. Using a *drosophila* model, a genetic screen has revealed that senataxin acts as a potent suppressor of C9orf72 DPR induced toxicity. But despite this evidence which suggests a commonality in the molecular pathways, the mechanistic basis of this discovery and role of senataxin has yet to be determined.

In this study, we attempted to 1) Characterize motor neuron dysfunction and neurotoxicity in SETX L389S$^{+/-}$ mice *in vivo* and *in vitro* using a primary neuron model 2) Generate an *in vitro* model to recapitulate studies which suggest senataxin is a potent suppressor of C9orf72 DPR toxicity. 3) Characterize subcellular localization of senataxin. 4) Investigate senataxin as an interactor of C9orf72 DPRs.

To determine if SETX L389S$^{+/-}$ mice display motor neuron dysfunction, we investigated nuclear membrane morphology by using L5 spinal cord sections from SETX L389S$^{+/-}$ mice. We documented nuclear membrane abnormalities by immunostaining sections with Ran and RanGAP1, nucleocytoplasmic transport factors. This suggests that abnormal nuclear membrane morphology could be the source of the defects that our lab has observed in nucleocytoplasmic trafficking, given that there's evidence of impaired nuclear pore complex. This in turn supports a mechanisms for the TDP-43 mislocalization our lab has also observed in ALS4 mice. These finding suggest shared pathological features with more common forms of ALS, such as in C9orf72-ALS[13]. Given these results, the RNA processing pathways that senataxin might normally regulate could be critical for maintaining the nuclear pore complex and nucleocytoplasmic trafficking.

Using the SETX L389S$^{+/-}$, primary cortical neurons grown in normal growth conditions have shown that mutations in SETX are sufficient to induce cell death. Additionally, to support these findings, an *in vitro* cerebellar granule neuron (CGN) model cultured in low potassium conditions, a model which mimics the effects of neurodegeneration, suggests that CGN expressing SETX L389S$^{+/-}$ mutation are also highly susceptible to cell death[37,38]. Primary cortical neurons transduced with SETX shRNA

exhibited an inability to tolerate reduced expression of senataxin. Despite only a ~50% knockdown of SETX at both the mRNA and protein levels, senataxin dosage reduction was sufficient to induce cell death. The sensitivity of neurons to non-physiological levels of senataxin and their inability to compensate for this gene dose insufficiency suggests that senataxin is an essential cell survival gene.

In an attempt to further characterize the localization of senataxin, we have determined through subcellular fractionation studies that endogenous senataxin has a prominent localization to the nucleolus. Although unexpected, based on previous independent findings which suggest senataxin displays a primarily nuclear localization, these results are not surprising, considering that Sen1p, the yeast orthologue of senataxin, has been found to play significant roles in the maintaining the integrity of the nucleolus[28]. Additionally, we have shown that EXOSC10, the enzymatic subunit of the nuclear exosome and known interactor of senataxin, has an almost exclusively nucleolar localization. This finding proposes that senataxin may have additional functions, which encompass regulating RNA processing and coordinating exosome function in the nucleolus.

A genetic screen in *Drosophila Melanogaster* has revealed a connection between senataxin and C9orf72, in which overexpression of the fly orthologue of SETX acts as a potent suppressor of DPR induced toxicity. This was established using both an $(G4C2)_{58}$-GFP and a GFP-GR_{50} C9orf72-ALS model. In an attempt to recapitulate these studies, several *in vitro* models were utilized, HEK293T cell line model, and two mouse primary

cortical neuron (PCN) models, from wildtype and C9orf72-450 BAC transgenic (C9-450B) mice.

HEK293T cells transfected with GR and wildtype PCN transduced with GR lentivirus proved to be toxic with little to no toxicity experienced in cells expressing GA. This corroborates independent findings which suggest that expression of GR but not GA is sufficient to induce cell death. Following this study, DPRs were co-expressed with either SETX siRNA or shRNA. Reduced expression of SETX in both HEK293T cells and PCN demonstrated an ability to exacerbate GR toxicity. To further evaluate the link between senataxin and C9orf72 and the ability for reduced expression of senataxin to exacerbate DPR induced toxicity, C9-450B transgenic mice, which express a human C9orf72 $(G_4C_2)_{450}$ repeat transgene, were used. Similar trends were observed in which PCN dissociated from these mice showed increased levels of neurotoxicity upon reduced SETX expression.

Although these finding support a connection between senataxin and C9orf72, overexpression of SETX in each of these models is necessary to show that senataxin is a suppressor of DPR induced toxicity. Unfortunately, due to the size of SETX, which exceeds the cloning and packaging capacity required for using a lentiviral transfer plasmid, this has not been plausible. Additional attempts have been made to overexpress SETX in neurons, in which our second ASL4 mouse model, Prp-SETX-R2136H transgenic model, shows increased levels of SETX RNA expression but insignificant increases at the protein level. This suggests that SETX expression is highly regulated, potentially due to an intolerance for levels greater than endogenous. An internally truncated mini-SETX

construct, which potentially could be cloned into a lentiviral vector, was also generated which retains both helicase and protein interaction domain, but this has seen limited success which includes mislocalization to the cytosol. Currently, our lab is still investigating possible solutions to this problem.

As part of a mechanistic study to determine how senataxin and C9orf72 are linked, we investigated a protein interaction between DPR proteins and SETX. Using co-immunoprecipitation, it was determined that senataxin displays preferential binding with GR. Although this interaction is resonant of RBPs such as TDP-43 and FUS which display a similar interaction, many of these proteins contain low complexity domains (LCD), for which senataxin does not. What could explain this GR interaction without the presence of a LCD? An interactome study identifying 202 GR and PR interactors has shown that 47 interactors were GR specific and 32.1% of total interactors did not contain a LCD, adding further support for this finding[18]. Interestingly, we have also determined that senataxin might exhibit an RNA-dependent interaction with GR, proposing a potential mechanism for this curious result. This function of senataxin to initiate an interaction through an RNA intermediate is additionally supported by evidence in which senataxin can interact with the nuclear exosome using a similar mechanism. As we look forward, we will further explore the functions of senataxin and define its role in the nucleolus. We will continue to characterize the significance of the observed DPR interaction as well as determine if senataxin interacts with SR splicing factors. As well, we will implement techniques such as CLIP-seq to define SETX RNA mediated interactions in order further characterize the role of senataxin in C9orf72-ALS.

MATERIALS AND METHODS

Generation of mouse model

SETX-L389S$^{+/-}$: This construct was generated by PCR amplification from murine BAC clone DNA (426D2). Site-directed mutagenesis was used to introduce the L389S substitution and was then cloned into a standard targeting vector (4317G9). This construct was then validated using DNA sequencing. Embryonic stem (ES) cell electroporation was followed by G418 selection, in which three SETX-L389S clones were found to be correctly integrated. One clone was selected to develop a chimera, by injection of a 3.5 day old blastocysts, to which two chimeric mice were selected and were used to produce F1 offspring. Breeding F1 mice with a homozygous CMV-Cre mice mediated removal of neo cassette which was validated by PCR.

C9orf72-450B: These mice were gifted to us from the Don Cleveland lab (University of California, San Diego) and their derivation was detailed in a previous publication[35].

siRNA/shRNA knock-down

RNA samples were isolated using Trizol (Life Technologies). Quantification of mRNA was performed using an Applied Biosystems 7500 Real Time (RT) Sequence Detection System. ABI Assays-on-Demand with TaqMan-based probes for human *SETX* (Hs00981138_m1), mouse Setx (Mm00616677_m1) and Gapdh (Mm99999915_g1) were shown to be highly specific with little to no cross reactivity. As the different primer-probe sets had similar amplification kinetics, comparative Ct (cycle threshold) was used to detect gene expression as previously described[36].

Plasmids and siRNA

For siRNA knockdown experiments, HEK293T cells were transiently transfected with predesigned Silencer Select siRNA to *SETX* (s22951) or a Scramble control (si-CRL) using RNAiMAX Reagent (Invitrogen) following manufacturers instruction. Unless otherwise stated, siRNA was used at a concentration of 10 nM. Details of the cloning and PCR amplification of the Flag-tagged SETX construct were outlined in our previous publication [28]. The Flag-hnRNPH expression construct was purchased from GeneCopoeia. All constructs generated by our group were validated by standard DNA Sanger sequencing prior to use. Plasmids such as pEGFPC-GR_{30}, pEGFPC-GA_{30}, pEGFPC-GP_{30}, pEGFPC-PA_{30}, pEGFPC-$PR_{30,}$ were generously gifted to us from Dr. Zheng Ying (College of Pharmaceutical Sciences, Soochow University, Suzhou, Jiangsu). Details can be found in their previous publication[15].

Primary cortical neuron (PCN) culture and lentivirus

Lentivirus was generated using HEK293FT cells. Cells were grown in DMEM high glucose (ThermoFisher Scientific) plus 10% FBS, 1X penicillin-streptomycin, non-essential amino acids, sodium pyruvate, and Geneticin. Cells were transfected at 90% confluency using Lipofectamine 2000 (ThermoFisher Scientific) in antibiotic-free media. After 48 hours, media was subjected to a 0.22 μM filter before virus was pelleted using sucrose gradient centrifugation at 22,000 RPM using an Optima L-80 XP Ultracentrifuge 1 (Beckman Coulter). Lentivirus was resuspended in PBS and stored at -80c until use.

Primary cortical neurons (PCN) were cultured from dissociated cortex of postnatal day 0-2 (P0-P2) mice. Dissociation was performed using Trypsin (T9935), Trypsin Inhibitor (T6522), and DNase I (Roche). Primary neurons were seeded onto plates coated with 0.1 mg/mL poly-D-lysine hydrobromide (P1024) and grown in complete medium

consisting of Neurobasal-A medium (Thermo Fisher Scientific) supplemented with 0.5 mM L-glutamine (ThermoFisher Scientific), 0.25% penicillin-streptomycin (Thermo Fisher Scientific), and 0.25% B-27 supplement (ThermoFisher Scientific).

Primary cerebellar granule neuron (CGN) culture

Cerebellar granule neurons (CGN) were cultured from dissociated cerebellum from postnatal day 7-8 (P7-P8) mice. Dissociation was performed using Trypsin (T9935), Trypsin Inhibitor (T6522), and DNase I (Roche). Primary neurons were seeded onto plates coated with 0.1 mg/mL poly-D-lysine hydrobromide (P1024) and grown in complete medium consisting of Neurobasal-A medium (ThermoFisher Scientific) supplemented with 0.5 mM L-glutamine (Thermofisher Scientific), 0.25% penicillin-streptomycin (Thermofisher Scientific), and 0.25% B-27 supplement (ThermoFisher Scientific) and 25 mM KCl. At day 14, neurons were subjected to potassium withdrawal, as previously described[37,38].

Culturing cell lines and transfection

Human Embryonic Kidney cells (HEK293T) were purchased from ATCC. Cell line was grown in DMEM high glucose (ThermoFisher Scientific) plus 10% FBS and 1X penicillin-streptomycin. Transfection was done using Lipofectamine 2000 (Invitrogen).

Western blot analysis

For sample preparation, cell lines or primary neurons were lysed with RIPA Buffer [(ThermoFisher Scientific) (25mM Tris HCl pH 7.6, 150mM NaCl, 1% NP-40, 1% sodium deoxycholate, 0.1% SDS)]. Cell lysates were subjected to sonication and then mixed with 10X sample reducing agent (Life Technologies) and 4X LDS sample buffer (Thermo Fisher Scientific). This was followed by heating at 70^{O}C for 10 minutes.

Separation of proteins was done with 8% or 4-12% Bis-Tris gel (ThermoFisher Scientific), and transferred onto polyvinylidene difluoride (PVDF) membrane. Membranes were blocked with 5% nonfat dry blotting milk in 1x PBST. Incubation of primary antibody (1:1000) was performed overnight at 4^{O}C and secondary antibody (1:5,000-1:10,000) was performed for 1 hour at room temperature. Following this, immunoreactivity was developed by chemiluminescence, HyGLO (Deville Scientific) and ECL prime (GE Healthcare) and visualized by autoradiography.

Propidium Iodide staining

Cells were stained with propidium iodide (PI), a membrane impermeable red-fluorescent dye which does not enter viable cells [Sigma-Aldrich (*P4864*)], 1:3,000 and Hoechst 33342 [ThermoFisher Scientific (H3570)] 1:10,000. Following 15 minute incubation in atmosphere of 5% CO_2 at 37 °C, confocal microscopy (Zeiss 780LSM) at 10x was used. 3 images were taken per well and each experiment was performed in at least triplicate. Quantification was completed with ImageJ software (NIH).

Lactose Dehydrogenase assay

Lactose Dehydrogenase (LDH) Cytotoxicity Colorimetric Assay (BioVision) reagents were prepared according to manufacturer's instructions. Cell lysis solution was added to control wells marked as high control and media was replaced with fresh media in wells marked as low control with respective cell media. Cells were then incubated for 20 minutes in atmosphere of 5% CO_2 at 37 °C. Following this, media from cells was added to respective LDH reagent and incubated at room temperature for 30 minutes. Following incubation, optical density was measured by microplate reader (Tecan) at 450nm and reference of 650nm. Quantification of LDH released (cell death) was calculated relative to

controls. Values were normalized to cell density using BCA protein assay kit (ThermoFischer Scienific).

Immunoprecipitation

Cell lysates were harvested from 6-well plates 48 hours post transfection using Pierce IP lysis Buffer (ThermoFisher Scientific) supplemented with protease (Roche) and phosphatase inhibitors (Roche). Following sonication and centrifugation at 12,000 RPM, cell lysates were subjected to 82.5ug of RNaseA per sample (Sigma #R4642) and pre-cleared using Protein G Dynabeads (ThermoFisher Scientific) for 1 hour at 4 degree on a rotator. Prior to immunoprecipitation, primary antibody was incubated with Dynabeads (ThermoFisher Scientific) for 2 hours at 4 degree on a rotator. Half of the cell lysate was immunoprecipitated using normal IgG, as a control.

Cell fractionation

Cells were trypsinized (Gemini) and harvested from five $15cm^2$ plates in a hypotonic buffer and subjected to cell lysis using a 15ml Dounce homogenizer, utilizing both tight and loose pestles. Lysates were centrifuged and cytosolic fractions were isolated. Nuclear fractions were suspended in 0.25mM sucrose solution and isolated using 0.35mM sucrose gradient centrifugation. Nuclear fractions were sonicated ($1/16^{th}$ probe, 25% amplitude, 10 seconds, 3 times) to release nucleoli. Following sonication, 0.88mM sucrose gradient centrifugation was used to isolate nucleolar pellet from nuclear fraction. Finally, 0.35mM sucrose gradient centrifugation was used to wash nucleoli pellet. Fractions were stored in cell lysis buffer (Cell Signaling)

Immunohistochemistry

Cryo-sections were generated by OCT-embedding and then cut to 25-µm. For immunostaining with Ran antibody, antigen retrieval using R-Universal Epitope Recovery Buffer (Electron Microscopy Science) was performed. Free floating spinal cord sections were incubated in a pressure cooker for 40 min. Sections were then cooled for 20 min before immunohistochemistry. RanGAP1 antibody was used without antigen retrieval. Sections were blocked in 5% BSA and 5% goat serum for 1 hour and incubated in primary antibody overnight at 4˚C. Sections were then incubated in secondary Alexafluor-conjugated antibody (Invitrogen) for 1 hour at room temperature and then mounted on slides using Fluoromount G (Electron Microscopy Sciences).

Antibodies

Cleaved Caspase 3 [Cell Signaling (#9664)], Beta Actin [Abcam (ab8226)], p-62 [Enzo (BML-PW9860-0100)], Senataxin [Bethyl (A301-104A), GFP [Santa Cruz (sc-9996)], EXOSC9 [Novus (NBP1-71702)], EXOSC10 [Novus (NBP1-32870)], alpha-tubulin [Cell Signaling (#3873)], Lamin A/C [Cell Signaling (#4777S)], Fibrillarin [GeneTex(GTX24566)], B23 [Proteintech (60096-1-Ig)], m2-Flag [Sigma(F7425)], RanGAP1 [Santa Cruz (sc-25630)], Ran (Thermofischer Scientific(# 610341)], TDP-43 [Protein Tech(12892-1-AP)], hnRNPH [Abcam(ab10374-50)]

Statistical Analysis

All graphs were generated using GraphPad Prism 7 software. Unless otherwise mentioned, statistical analysis was done using unpaired two-tailed t test (student's t-test), and the results are shown as mean ± SEM. p values of <0.05 were considered statistically significant. Asterisks indicate the following p values: *p< 0.05, **p< 0.01, ***p< 0.001

FIGURES

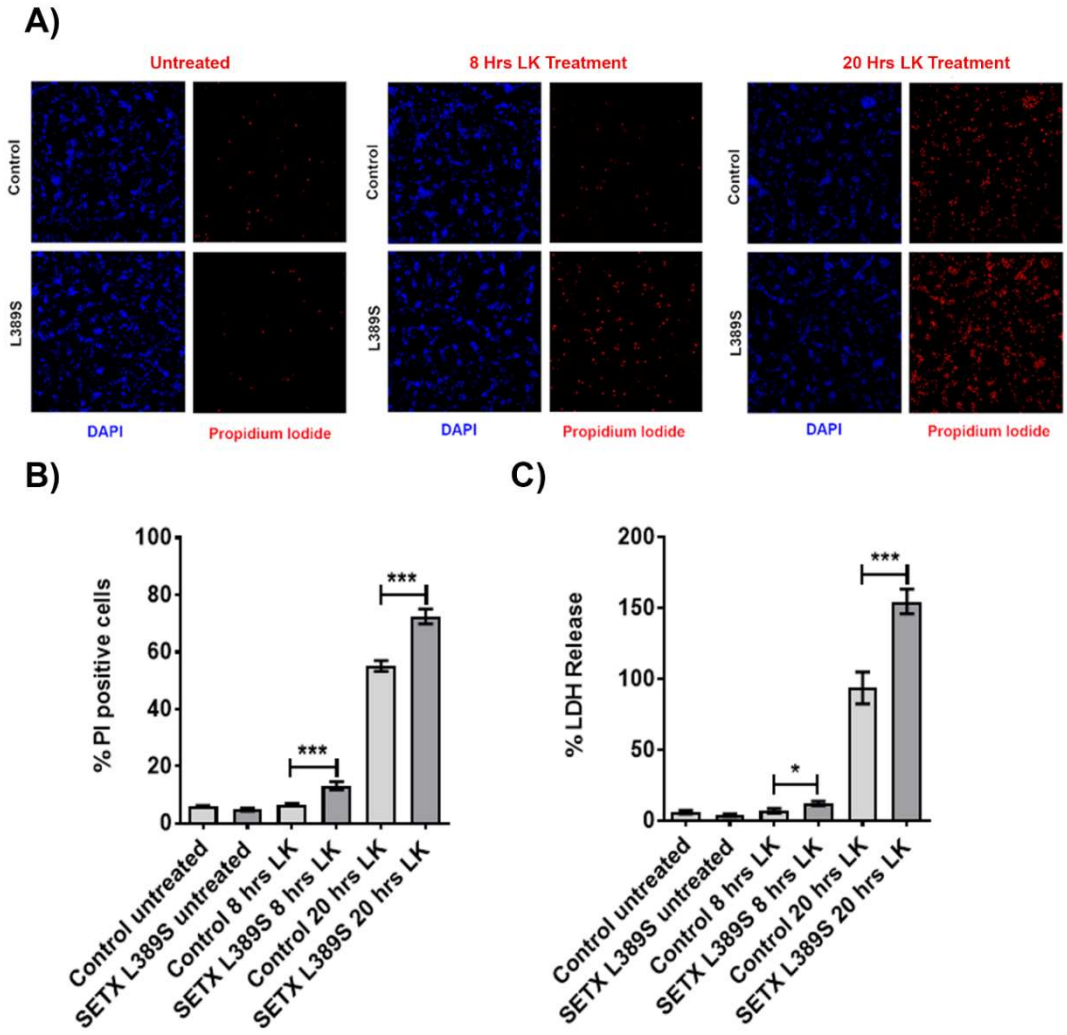

Figure 1: SETX L389S cerebellar granule neurons (CGN) exhibit increased susceptibility to cell death

A. Propidium Iodide (PI) stained and DAPI counterstained cerebellar granule neurons (CGN) from SETX L389S$^{+/-}$ and control littermates subjected to potassium withdrawal, from medium containing high potassium (HK) to low potassium (LK) for 0, 8 and 20 hours.
B. Quantification of propidium iodide stained cerebellar granule neurons (CGN) from SETX L389S$^{+/-}$ and control littermates subjected to potassium withdrawal, from medium containing high (HK) to low (LK) potassium for 0, 8 and 20 hours (n=3, ***$p < 0.001$, student's t-test, error bars=s.e.m.).
C. Quantification of lactate dehydrogenase (LDH) release using cerebellar granule neurons (CGN) from SETX L389S$^{+/-}$ and control littermates subjected to potassium withdrawal, from medium containing high potassium (HK) to low potassium (LK) for 0, 8 and 20 hours (n=3, *$p < 0.05$, ***$p < 0.001$, student's t-test, error bars=s.e.m.)

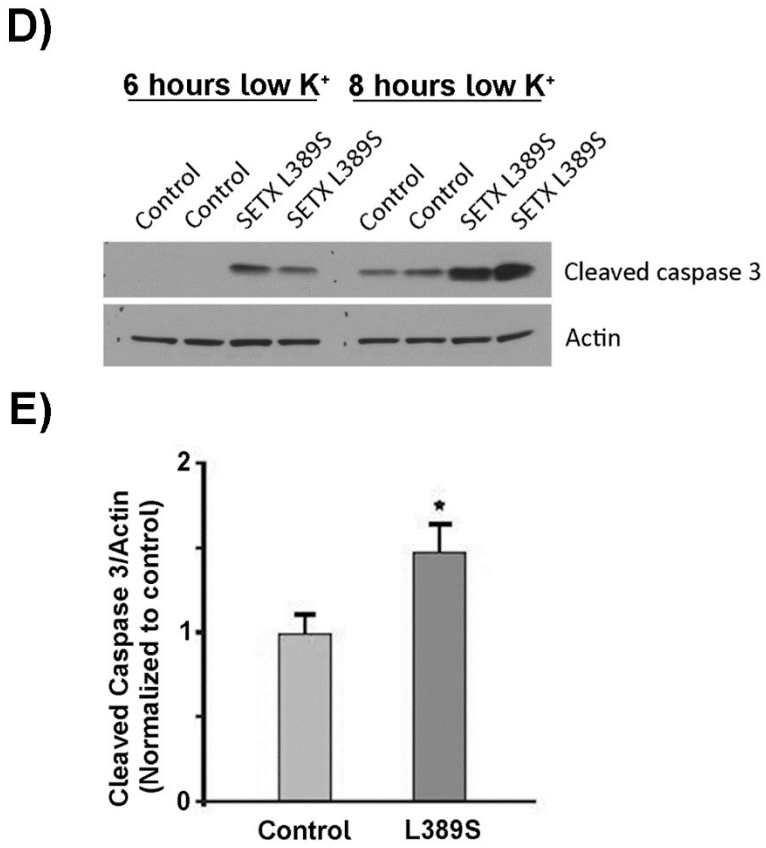

Figure 1: **SETX L389S cerebellar granule neurons (CGN) exhibit increased susceptibility to cell death, Continued**

D. Western blot of cleaved caspase 3 and actin loading control. Cerebellar granule neurons (CGN) from SETX L389S$^{+/-}$ and control littermates were subjected to potassium withdrawal, from medium containing high potassium (HK) to low potassium (LK) for 6 and 8 hours.

E. Quantification of cleaved caspase 3 normalized to actin levels. Cerebellar granule neurons (CGN) from SETX L389S$^{+/-}$ and control littermates were subjected to potassium withdrawal, from medium containing high potassium (HK) to low potassium (LK) for 6 and 8 hours. (n=9, *$p < 0.05$, student's t-test, error bars=s.e.m.).

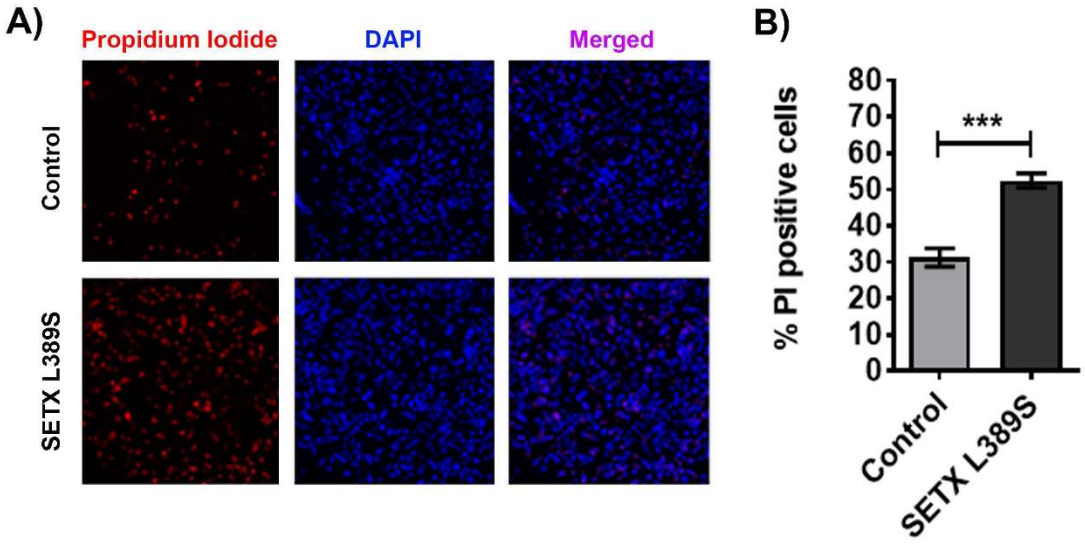

Figure 2: SETX L389S primary cortical neurons (PCN) exhibit increased susceptibility to cell death

A) Propidium Iodide (PI) stained and DAPI counterstained primary cortical neurons (PCN) from SETX L389S$^{+/-}$ and control littermates

B) Quantification of propidium iodide stained primary cortical neurons (PCN) from SETX L389S$^{+/-}$ and control mice (n=3, ***$p < 0.001$, students t-test, error bars=s.e.m.).

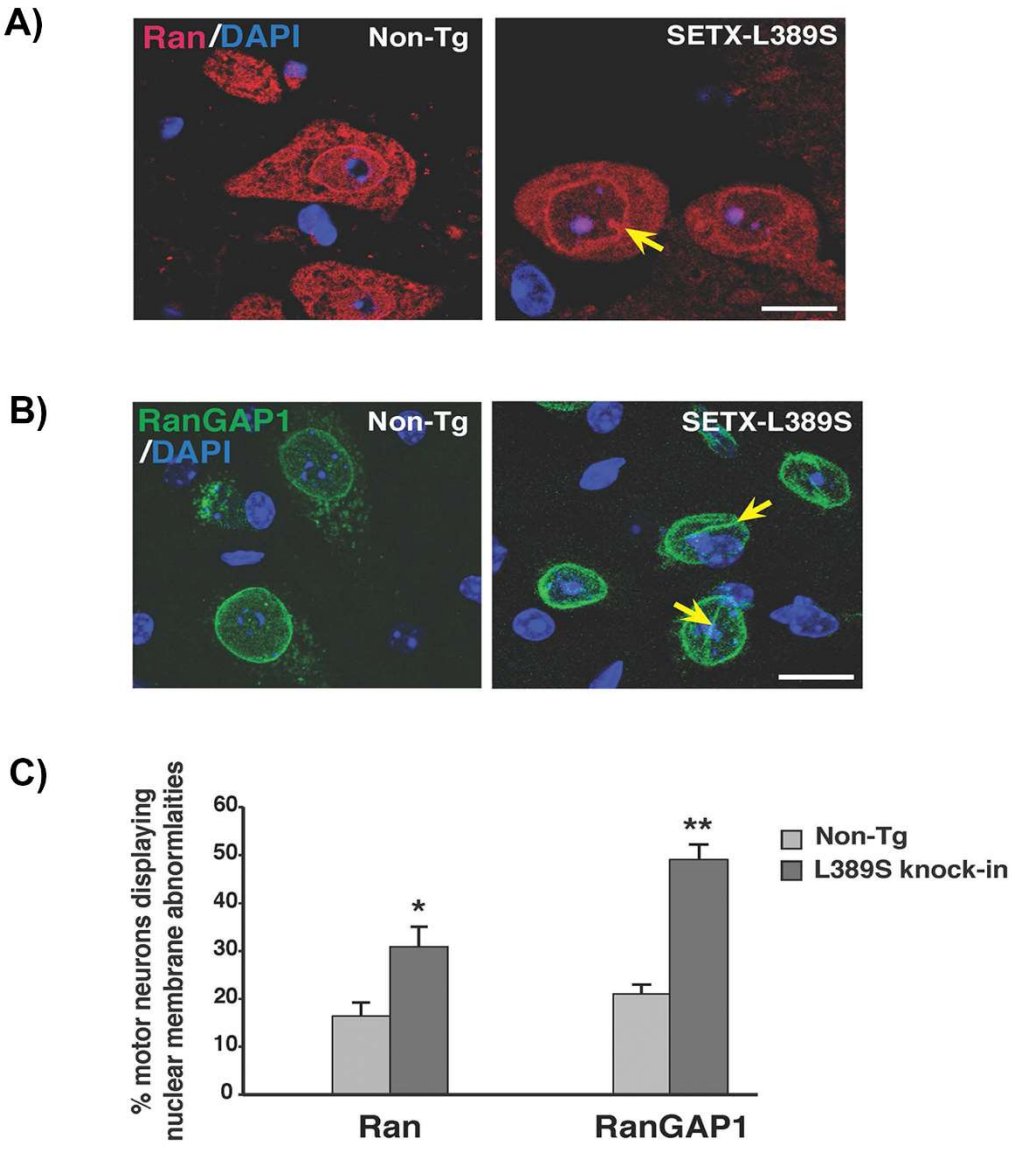

Figure 3: SETX L389S motor neurons display defects to nuclear membrane morphology

A. L5 spinal cord motor neurons acquired from 11.5 month old SETX L389S$^{+/-}$ and control littermates. Sections are immunostained for Ran and nuclear counterstained with DAPI.
B. L5 spinal cord motor neurons acquired from 11.5 month old SETX L389S$^{+/-}$ and control littermates. Sections are immunostained for RanGAP1 and nuclear counterstained with DAPI.
C. Quantification of Ran and RanGAP1 immunostained motor neurons positive for nuclear membrane abnormalities (n=3, 50-80 cells/mouse *$p < 0.05$, **$p < 0.01$, student's t-test, error bars=s.e.m.).

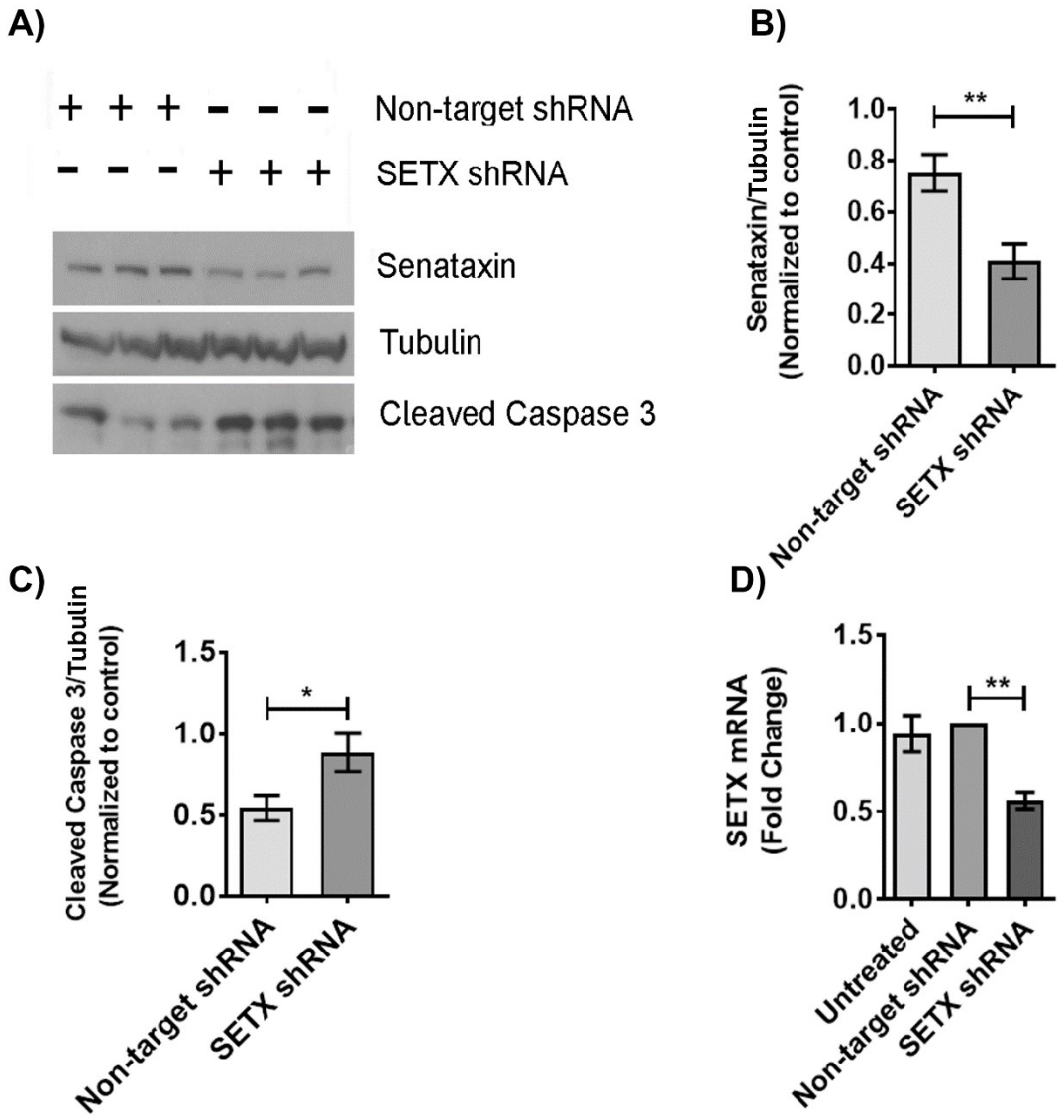

Figure 4: Reduced expression of SETX induces cell death in primary cortical neurons

A. Western blot of cleaved caspase 3, senataxin and tubulin loading control. Primary cortical neurons (PCN) from C57Bl6/j mice transduced with SETX and non-target shRNA.
B. Quantification of senataxin normalized to tubulin levels. Primary cortical neurons (PCN) from C57Bl6/j mice transduced with SETX and non-target shRNA (n=5, $**p < 0.01$, student's t-test, error bars=s.e.m.).
C. Quantification of cleaved caspase 3 normalized to tubulin levels. Primary cortical neurons (PCN) from C57Bl6/j mice transduced with SETX and non-target shRNA (n=5, $*p < 0.05$, student's t-test, error bars=s.e.m.).
D. Quantification of quantitative PCR (qPCR) measured as fold-change of SETX mRNA. Primary cortical neurons (PCN) from C57Bl6/j mice transduced with SETX and non-target shRNA (n=2, 3 technical replicates each, $**p < 0.01$, student's t-test, error bars=s.e.m.)

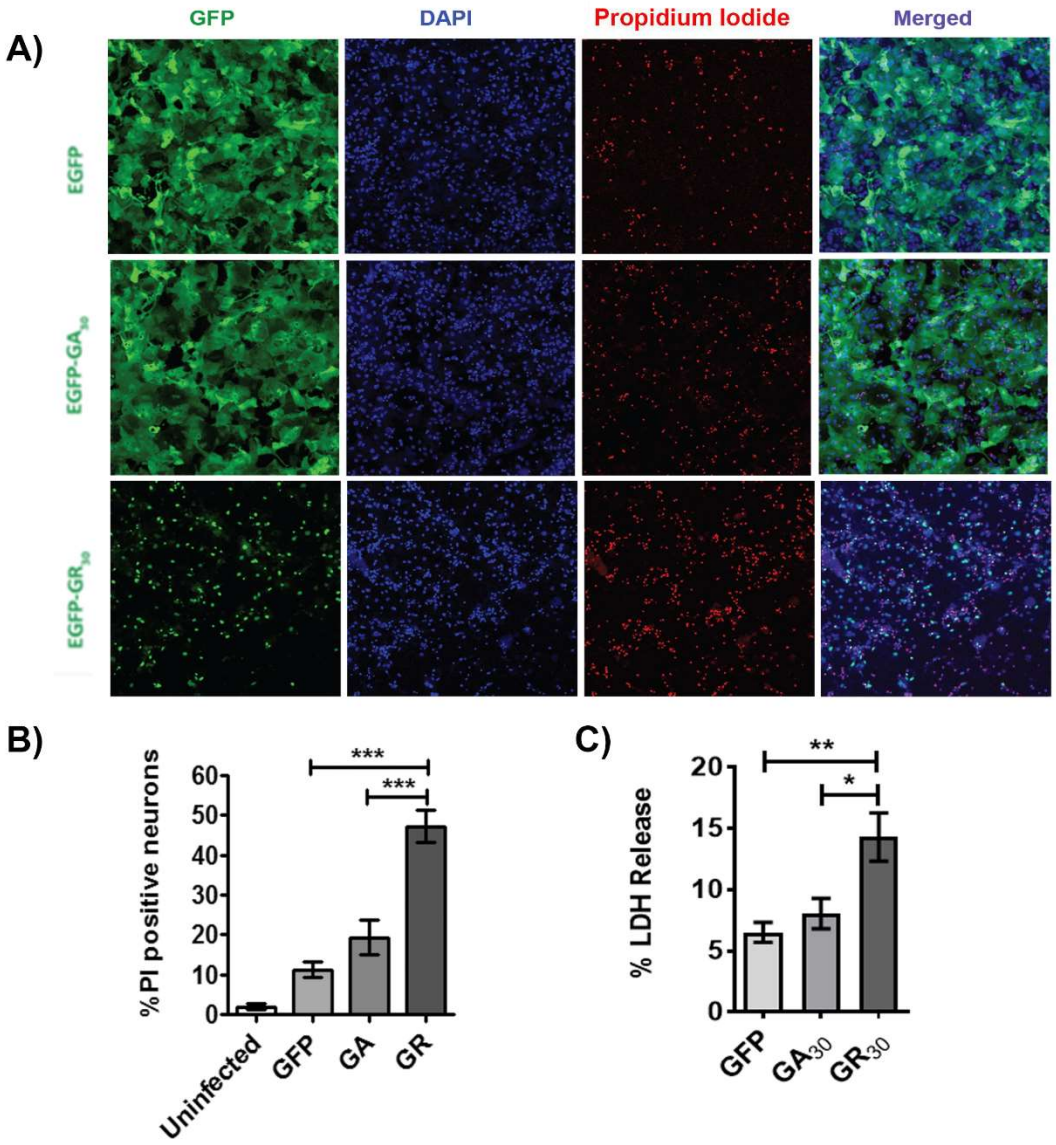

Figure 5: C9orf72 poly-GR, but not poly-GA, induces toxicity in primary cortical neurons

A. Propidium Iodide (PI) stained and DAPI counterstained primary cortical neurons (PCN) from C57Bl6/j mice transduced with pEGFP control, pEGFP-GA_{30} or pEGFP-GR_{30}.

B. Quantification of propidium iodide stained primary cortical neurons (PCN) from C57Bl6/j mice transduced with pEGFP control, pEGFP-GA_{30} or pEGFP-GR_{30} (n=7, ***$p < 0.001$, student's t-test, error bars=s.e.m.).

C. Quantification of lactate dehydrogenase (LDH) release using primary cortical neurons (PCN) from C57Bl6/j mice transduced with pEGFP control, pEGFP-GA_{30} or pEGFP-GR_{30} (PCN) (n=4, *$p < 0.05$, **$p < 0.01$, student's t-test, error bars=s.e.m.)

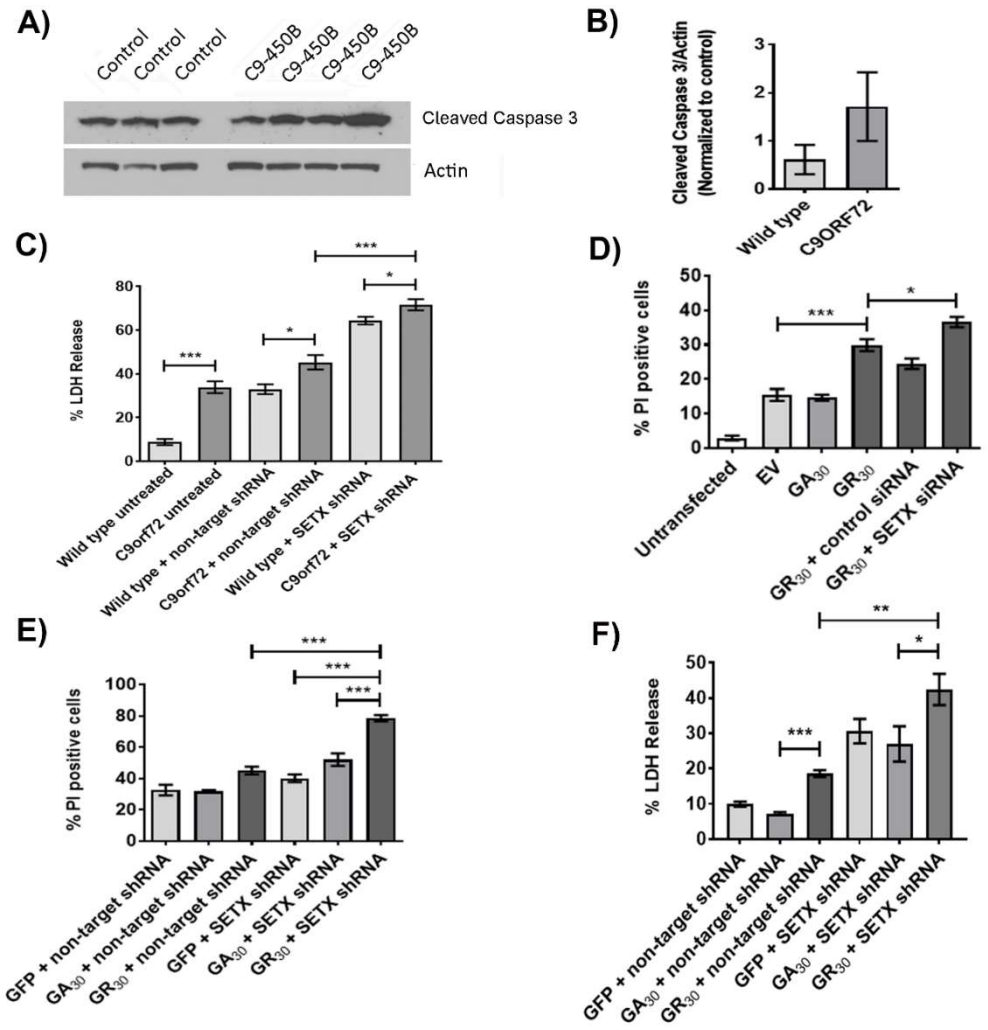

Figure 6: Toxicity induced by various C9orf72 models is exacerbated by reduced expression of SETX

A. Western blot of cleaved caspase 3 and actin loading control. Primary cortical neurons (PCN) from C9-450B and control littermates.
B. Quantification of cleaved caspase 3 normalized to actin levels. Primary cortical neurons (PCN) from C9-450B and control littermates (n=3, student's t-test, error bars=s.e.m.
C. Quantification of lactate dehydrogenase (LDH) release using primary cortical neurons (PCN) from C9-450B mice and control littermates transduced with either SETX shRNA or control non-target shRNA (n=3, $*p < 0.05$, $***p < 0.001$, student's t-test, error bars=s.e.m.).
D. Quantification of propidium iodide (PI) stained HEK293T cells transfected with pEGFP control, pEGFP-GA_{30} or pEGFP-GR_{30} and either SETX siRNA or control siRNA (3 technical replicates, $*p < 0.05$, $***p < 0.001$, student's t-test, error bars=s.e.m.).
E. Quantification of propidium iodide (PI) stained primary cortical neurons (PCN) from C57Bl6/j mice transduced with pEGFP control, pEGFP-GA_{30} or pEGFP-GR_{30} and either SETX shRNA or control non-target shRNA (3 technical replicates, $***p < 0.001$, student's t-test, error bars=s.e.m.).
F. Quantification of lactate dehydrogenase (LDH) release using primary cortical neurons (PCN) from C57Bl6/j mice transduced with pEGFP control, pEGFP-GA_{30} or pEGFP-GR_{30} and either SETX shRNA or control non-target shRNA (3 technical replicates, $*p < 0.05$, $**p < 0.01$, $***p < 0.001$, student's t-test, error bars=s.e.m.).

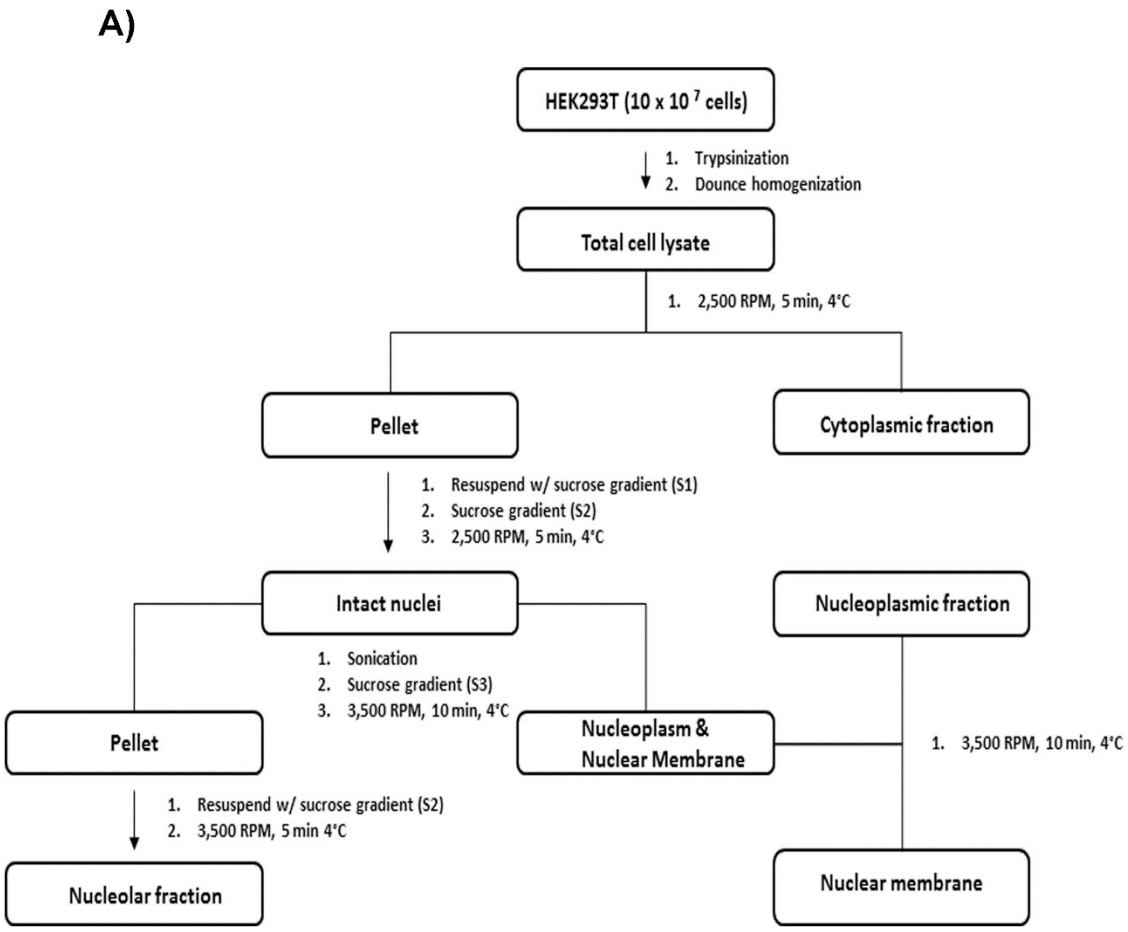

Figure 7: Senataxin shows prominent nucleolar localization as revealed by sub-cellular fractionation

A. Approximately 10 x 10^7 HEK293T cells were fractionated into four distinct fractions, including cytoplasm, nuclear membrane, nucleoplasm, and the nucleolus. S1 =0.25mM sucrose gradient, S2=0.35mM sucrose gradient, and S3=0.88mM sucrose gradient.

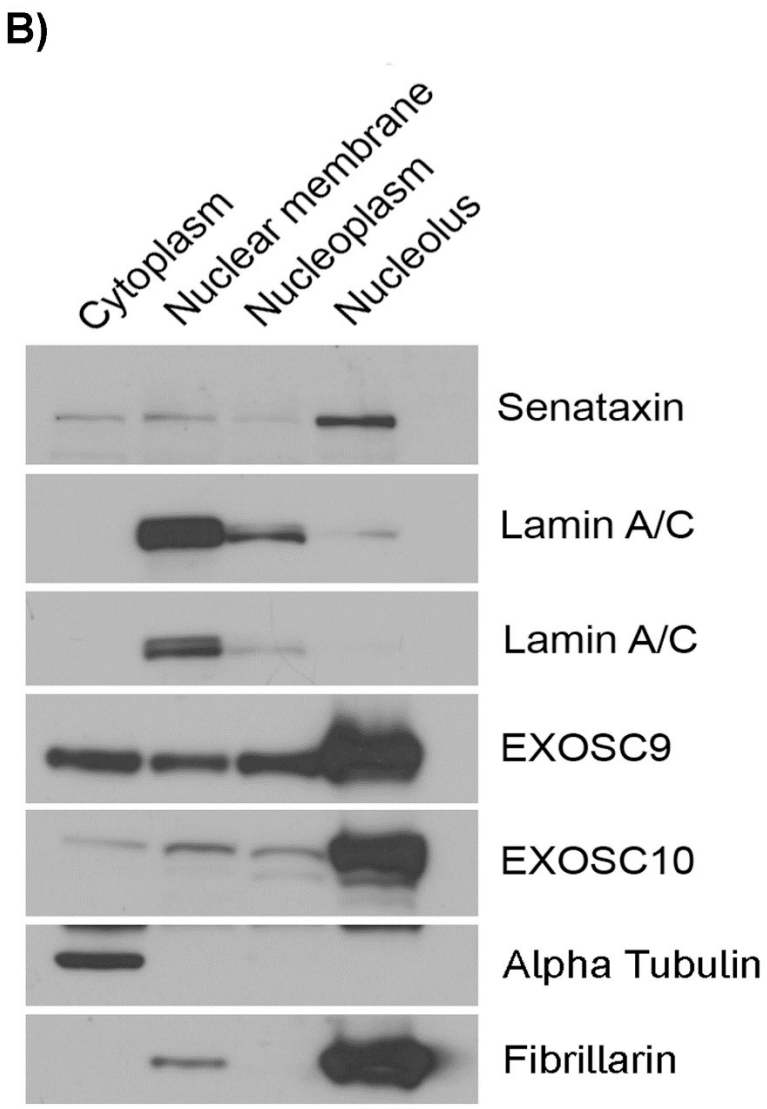

Figure 7: Senataxin shows prominent nucleolar localization as revealed by sub-cellular fractionation, Continued

B. Western blot of sub-cellular fractionation. HEK293T cells were fractioned into cytoplasmic, nuclear membrane, nucleoplasmic, and nucleolar fractions. In addition to senataxin and interactors EXOSC9 and EXOSC10, fractions were analyzed using different subcellular markers. These include cytoplasmic marker Alpha tubulin, nuclear membrane marker Lamin A/C, and nucleolar marker Fibrillarin.

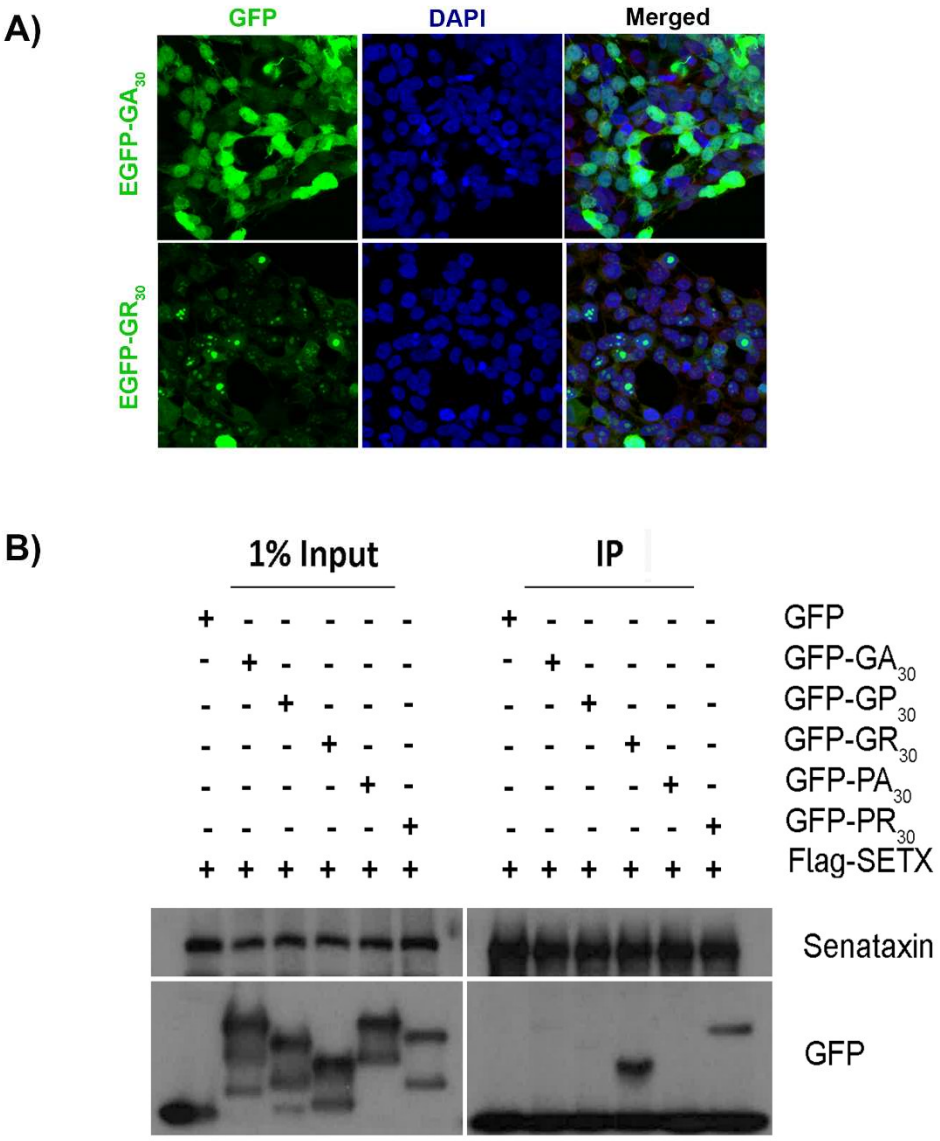

Figure 8: C9orf72 poly-GR localizes to the nucleolus and interacts with senataxin

A) HEK293T cells were transfected with either pEGFP-GR_{30} or pEGFP-GA_{30}. Analysis of sub-cellular localization was determined using GFP and cells were counterstained with DAPI.

B) HEK293T cells were transfected with Flag-SETX and either pEGFP-GR_{30}, pEGFP-GA_{30}, pEGFP-GP_{30}, pEGFP-PA_{30}, pEGFP-PR_{30} or pEGFP control. Cells were then subjected to immunoprecipitation (IP) with anti-Flag antibody or IgG control antibody. Western blot analysis with indicated antibodies was then performed.

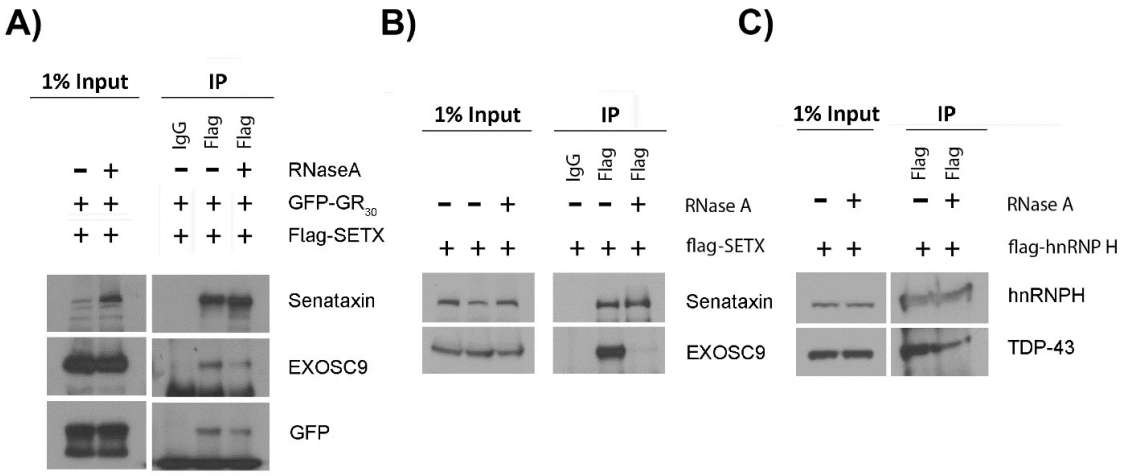

Figure 9: Senataxin displays RNA-mediated interactions with C9orf72 poly-GR and exosome

A) HEK293T cells were transfected with Flag-SETX and pEGFP-GR_{30}. Half of the lysate was treated with RNaseA and then subjected to immunoprecipitation (IP) with anti-Flag antibody. Western blot analysis with indicated antibodies was then performed.

B) HEK293T cells were transfected with Flag-SETX. Half of the lysate was treated with RNaseA and then subjected to immunoprecipitation (IP) with anti-Flag antibody. Western blot analysis with indicated antibodies was then performed.

C) HEK293T cells were transfected with Flag-hnRNPH. Half of the lysate was treated with RNaseA and then subjected to immunoprecipitation (IP) with anti-Flag antibody. Western blot analysis with indicated antibodies was then performed

REFERENCES

1. Vance, C., Al-Chalabi, A., Ruddy, D., Smith, B.N., Hu, X., Sreedharan, J., Siddique, T., Schelhaas, H.J., Kusters, B., Troost, D., Bass, F., De Jong, V. & Shaw, C.E. Familial amyotrophic lateral sclerosis with frontotemporal dementia is linked to a locus on chromosome 9p13.2-21.3. *Brain* **129**, 868-876 (2006).

2. Taylor, J.P., Brown, R.H., Jr. & Cleveland, D.W. Decoding ALS: from genes to mechanism. *Nature* **539**, 197-206 (2016).

3. Harms, M.B. & Baloh, R.H. Clinical neurogenetics: amyotrophic lateral sclerosis. *Neurologic clinics* **31**, 929-950 (2013).

4. Renton, A.E., Majounie, E., Waite, A., Simon-Sanchez, J., Rollinson, S., Gibbs, J.R., Schymick, J.C., Laaksovirta, H., Van Swieten, J.C., Myllykangas, L., Kalimo, H., Paetau, A., Abramzon, Y., Remes, A.M., Kaganovich, A., Scholz, S.W., Duckworth, J., Ding, J., Harmer, D.W., Hernandez, D.G., Johnson, J.O., Mok, K., Ryten, M., Trabzuni, D., Guerreiro, R.J., Orrell, R.W., Neal, J., Murray, A., Pearson, J., Jansen, I.E., Sondervan, D., Seelaar, H., Blake, D., Young, K., Halliwell, N., Callister, J., Toulson, G., Richardson, A., Gerhard, A., Snowden, J., Mann, D., Neary, D., Nalls, M.A., Peuralinna, T., Jansson, L., Isoviita, V. Kaivorinne, A., Hölttä-Vuori, M., Ikonen, E., Sulkava, R., Benatar, M., Wuu, J., Chio, A., Restagno, G., Borghero, G,. Sabatelli, M., Heckerman, D., Rogaeva, E., Zinman, L., Rothstein, J., Sendtner, M,. Drepper, C., Eichler, E.E., Alkan, C. Abdullaev, Z., Pack, S.D., Dutra, A., Pak, E., Hardy, J., Singleton, A., Williams, N.M., Heutink, P., Pickering-Brown, S., Morris, H.R., Tienari, P.J. & Traynor, B.J. A hexanucleotide repeat expansion in C9ORF72 is the cause of chromosome 9p21-linked ALS-FTD. *Neuron* **72**, 257-268 (2011).

5. Majounie, E., Renton, A.E., Mok, K., Dopper, E.G., Waite, A., Rollinson, S., Chiò, A., Restagno, G., Nicolaou, N., Simon-Sanchez, J., Van Swieten, J.C., Abramzon, Y., Johnson, J.O., Sendtner, M., Pamphlett, R., Orrell, R.W., Mead, S., Sidle, K.C., Houlden, H., Rohrer, J.D., Morrison, K.E., Pall, H., Talbot, K., Ansorge, O., Hernandez, D.G., Arepalli, S., Sabatelli, M., Mora, G., Corbo, M., Giannini, F., Calvo, A., Englund, E., Borghero, G., Floris, G.L., Remes, A.M., Laaksovirta, H., McCluskey, L., Trojanowski, J.Q., Van Deerlin, V.M., Schellenberg, G.D., Nalls, M.A., Drory, V.E., Lu, C.S., Yeh, T.H., Ishiura, H., Takahashi, Y., Tsuji, S., Le Ber, I., Brice, A., Drepper, C., Williams, N., Kirby, J., Shaw, P., Hardy, J., Tienari, P.J., Heutink, P., Morris, H.R., Pickering-Brown, S. & Traynor, B.J. Frequency of the C9orf72 hexanucleotide repeat expansion in patients with amyotrophic lateral sclerosis and frontotemporal dementia: a cross-sectional study. *Lancet Neurol* **11**, 323-330 (2012).

6. DeJesus-Hernandez, M., Mackenzie, I.R., Boeve, B.F., Boxer, A.L., Baker, M., Rutherford, N.J., Nicholson, A.M., Finch, N.A., Flynn, H., Adamson, J., Kouri, N., Wojtas, A., Sengdy, P., Hsiung, G.Y., Karydas, A., Seeley, W.W., Josephs, K.A., Coppola, G., Geschwind, D.H., Wszolek, Z.K., Feldman, H., Knopman, D.S., Petersen, R.C., Miller, B.L., Dickson, D.W., Boylan, K.B., Graff-Radford, N.R. & Rademakers, R. Expanded GGGGCC hexanucleotide repeat in noncoding region of C9ORF72 causes chromosome 9p-linked FTD and ALS. *Neuron* **72**, 245-256 (2011).

7. Mizielinska, S. & Isaacs, A.M. C9orf72 amyotrophic lateral sclerosis and frontotemporal dementia: gain or loss of function? *Current opinion in neurology* **27**, 515-523 (2014).

8. Zu, T., Liu, Y., Bañez-Coronel, M., Reid, T., Pletnikova, O., Lewis, J., Miller, T.M., Harms, M.B., Falchook, A.E., Subramony, S.H., Ostrow, L.W., Rothstein, J.D., Troncoso, J.C. & Ranum, L.P.W. RAN proteins and RNA foci from antisense transcripts in C9ORF72 ALS and frontotemporal dementia. *Proc Natl Acad Sci U S A* **110**, E4968-4977 (2013).

9. Zu, T., Gibbens, B., Doty, N.S., Gomes-Pereira, M., Huguet, A., Stone, M.D., Margolis, J., Peterson, M., Markowski, T.W., Ingram, M.A., Nan, Z., Forster, C., Low, W.C., Schoser, B., Somia, N.V., Clark, H.B., Schmechel, S., Bitterman, P.B., Gourdon, G., Swanson, M.S., Moseley, M. & Ranum L.P. Non-ATG-initiated translation directed by microsatellite expansions. *Proc Natl Acad Sci U S A* **108**, 260-265 (2011).

10. Cleary, J.D. & Ranum, L.P. Repeat-associated non-ATG (RAN) translation in neurological disease. *Hum Mol Genet* **22**, R45-51 (2013).

11. Freibaum, B.D. & Taylor, J.P. The Role of Dipeptide Repeats in C9ORF72-Related ALS-FTD. *Frontiers in molecular neuroscience* **10**, 35 (2017).

12. Ash, P.E., Bieniek, K.F., Gendron, T.F., Caulfield, T., Lin, W.L., Dejesus-Hernandez, M., Van Blitterswijk, M.M., Jansen-West, K., Paul, J.W., Rademakers, R., Boylan, K.B., Dickson, D.W. & Petrucelli, L. Unconventional translation of C9ORF72 GGGGCC expansion generates insoluble polypeptides specific to c9FTD/ALS. *Neuron* **77**, 639-646 (2013).

13. Freibaum, B.D., Lu, Y., Lopez-Gonzalez, R., Kim, N.C., Almeida, S., Lee, K.H., Badders, N., Valentine, M., Miller, B.L., Wong, P.C., Petrucelli, L., Kim, H.J., Gao, F.B. & Taylor, J.P. GGGGCC repeat expansion in C9orf72 compromises nucleocytoplasmic transport. *Nature* **525**, 129-133 (2015).

14. Mizielinska, S., Grönke, S., Niccoli, T., Ridler, C.E., Clayton, E.L., Devoy, A., Moens, T., Norona, F.E., Woollacott, I.O.C., Pietrzyk, J., Cleverley, K., Nicoll, A.J., Pickering-Brown, S., Dols, J., Cabecinha, M., Hendrich, O., Fratta, P., Fisher, E.M.C., Partridge, L. & Isaacs, A.M. C9orf72 repeat expansions cause neurodegeneration in Drosophila through arginine-rich proteins. *Science* **345**, 1192-1194 (2014).

15. Tao, Z., Wang, H., Xia, Q., Li, K., Li, K., Jiang, X., Xu, G., Wang, G. & Ying, Z. Nucleolar stress and impaired stress granule formation contribute to C9orf72 RAN translation-induced cytotoxicity. *Hum Mol Genet* **24**, 2426-2441 (2015).

16. Wen, X., Tan, W., Westergard, T., Krishnamurthy, K., Markandaiah, S.S., Shi, Y., Lin, S., Shneider, N.A., Monaghan, J., Pandey, U.B., Pasinelli, P., Ichida, J.K. & Trotti, D. Antisense proline-arginine RAN dipeptides linked to C9ORF72-ALS/FTD form toxic nuclear aggregates that initiate in vitro and in vivo neuronal death. *Neuron* **84**, 1213-1225 (2014).

17. Kwon, I., Xiang, S., Kato, M., Wu, L., Theodoropoulos, P., Wang, T., Kim, J., Yun, J., Xie, Y. & McKnight, S.L. Poly-dipeptides encoded by the C9orf72 repeats bind nucleoli, impede RNA biogenesis, and kill cells. *Science* **345**, 1139-1145 (2014).

18. Lee, K.H., Zhang, P., Kim, H.J., Mitrea, D.M., Sarkar, M., Freibaum, B.D., Cika, J., Coughlin, M., Messing, J., Molliex, A., Maxwell, B.A., Kim, N.C., Temirov, J., Moore, J., Kolaitis, R.M., Shaw, T.I., Bai, B., Peng, J., Kriwacki, R.W. & Taylor, J.P. C9orf72 Dipeptide Repeats Impair the Assembly, Dynamics, and Function of Membrane-Less Organelles. *Cell* **167**, 774-788.e717 (2016).

19. Lin, Y., Mori, E., Kato, M., Xiang, S., Wu, L., Kwon, I. & McKnight, S.L. Toxic PR Poly-Dipeptides Encoded by the C9orf72 Repeat Expansion Target LC Domain Polymers. *Cell* **167**, 789-802.e712 (2016).

20. Yin, S., Lopez-Gonzalez, R., Kunz, R.C., Gangopadhyay, J., Borufka, C., Gygi, S.P., Gao, F.B. & Reed, R. Evidence that C9ORF72 Dipeptide Repeat Proteins Associate with U2 snRNP to Cause Mis-splicing in ALS/FTD Patients. *Cell Rep* **19**, 2244-2256 (2017).

21. Polymenidou, M., Lagier-Tourenne, C., Hutt, KR., Huelga, S.C., Moran, J., Liang, T.Y., Ling, S.C., Sun, E., Wancewicz, E., Mazur, C., Kordasiewicz, H., Sedaghat, Y., Donohue, J.P., Shiue, L., Bennett, C.F., Yeo, G.W. & Cleveland, D.W. Long pre-mRNA depletion and RNA missplicing contribute to neuronal vulnerability from loss of TDP-43. *Nat Neurosci* **14**, 459-468 (2011).

22. Ling, J.P., Pletnikova, O., Troncoso, J.C. & Wong, P.C. TDP-43 repression of nonconserved cryptic exons is compromised in ALS-FTD. *Science* **349**, 650-655 (2015).

23. Bennett, C.L. & La Spada, A.R. Unwinding the role of senataxin in neurodegeneration. *Discovery medicine* **19**, 127-136 (2015).

24. Chen, Y.Z., Bennett, C.L., Huynh, H.M., Blair, I.P., Puls, I., Irobi, J., Dierick, I., Abel, A., Kennerson, M.L., Rabin, B.A., Nicholson, G.A., Auer-Grumbach, M., Wagner, K., De Jonghe, P., Griffin, J.W., Fischbeck, K.H., Timmerman, V., Cornblath, D.R. & Chance, P.F. DNA/RNA helicase gene mutations in a form of juvenile amyotrophic lateral sclerosis (ALS4). *American journal of human genetics* **74**, 1128-1135 (2004).

25. Moreira, M.C., Klur, S., Watanabe, M., Németh, A.H., Le Ber, I., Moniz, J.C., Tranchant, C., Aubourg, P., Tazir, M., Schöls, L., Pandolfo, M., Schulz, J.B., Pouget, J., Calvas, P., Shizuka-Ikeda, M., Shoji, M., Tanaka, M., Izatt, L., Shaw, C.E., M'Zahem, A., Dunne, E., Bomont, P., Benhassine, T., Bouslam, N., Stevanin, G., Brice, A., Guimarães, J., Mendonça, P., Barbot, C., Coutinho, P., Sequeiros, J., Dürr, A., Warter, J.M. & Koenig, M. Senataxin, the ortholog of a yeast RNA helicase, is mutant in ataxia-ocular apraxia 2. *Nat Genet* **36**, 225-227 (2004).

26. Suraweera, A., Lim, Y., Woods, R., Birrell, G.W., Nasim, T., Becherel, O.J. & Lavin, M.F. Functional role for senataxin, defective in ataxia oculomotor apraxia type 2, in transcriptional regulation. *Hum Mol Genet* **18**, 3384-3396 (2009).

27. Skourti-Stathaki, K., Proudfoot, N.J. & Gromak, N. Human senataxin resolves RNA/DNA hybrids formed at transcriptional pause sites to promote Xrn2-dependent termination. *Mol Cell* **42**, 794-805 (2011).

28. Chen, Y.Z., Hashemi, S.H., Anderson, S.K., Huang, Y., Moreira, M.C., Lynch, D.R., Glass, I.A., Chance, P.F. & Bennett, C.L. Senataxin, the yeast Sen1p orthologue: characterization of a unique protein in which recessive mutations cause ataxia and dominant mutations cause motor neuron disease. *Neurobiol Dis* **23**, 97-108 (2006).

29. Wagschal, A., Rousset, E., Basavarajaiah, P., Contreras, X., Harwig, A., Laurent-Chabalier, S., Nakamura, M., Chen, X., Zhang, K., Meziane, O., Boyer, F., Parrinello, H., Berkhout, B., Terzian, C., Benkirane, M. & Kiernan, R. Microprocessor, Setx, Xrn2, and Rrp6 co-operate to induce premature termination of transcription by RNAPII. *Cell* **150**, 1147-1157 (2012).

30. Richard, P., Feng, S. & Manley, J.L. A SUMO-dependent interaction between Senataxin and the exosome, disrupted in the neurodegenerative disease AOA2, targets the exosome to sites of transcription-induced DNA damage. *Genes Dev* **27**, 2227-2232 (2013).

31. Schmid, M. & Jensen, T.H. The exosome: a multipurpose RNA-decay machine. *Trends Biochem Sci* **33**, 501-510 (2008).

32. Bennett, C.L., Chen, Y., Vignali, M., Lo, R.S., Mason, A.G., Unal, A., Huq Saifee, N.P., Fields, S. & La Spada, A.R. Protein interaction analysis of senataxin and the ALS4 L389S mutant yields insights into senataxin post-translational modification and uncovers mutant-specific binding with a brain cytoplasmic RNA-encoded peptide. *PLoS One* **8**, e78837 (2013).

33. Kenna, K.P., McLaughlin, R.L., Byrne, S., Elamin, M., Heverin, M., Kenny, E.M., Cormican, P., Morris, D.W., Donaghy, C.G., Bradley, D.G. & Hardiman, O. Delineating the genetic heterogeneity of ALS using targeted high-throughput sequencing. *Journal of medical genetics* **50**, 776-783 (2013).

34. Cady, J., Allred, P., Bali, T., Pestronk, A., Goate, A., Miller, T.M., Mitra, R.D., Ravits, J., Harms, M.B. & Baloh, R.H. Amyotrophic lateral sclerosis onset is influenced by the burden of rare variants in known amyotrophic lateral sclerosis genes. *Ann Neurol* **77**, 100-113 (2015).

35. Jiang, J., Zhu, Q., Gendron, T.F., Saberi, S., McAlonis-Downes, M., Seelman, A., Stauffer, J.E., Jafar-Nejad, P., Drenner, K., Schulte, D., Chun, S., Sun, S., Ling, S.C., Myers, B., Engelhardt, J., Katz, M., Baughn, M., Platoshyn, O., Marsala, M., Watt, A., Heyser, C.J., Ard, M.C., De Muynck, L., Daughrity, L.M., Swing, D.A., Tessarollo, L., Jung, C.J., Delpoux, A., Utzschneider, D.T., Hedrick, S.M., de Jong, P.J., Edbauer, D., Van Damme, P., Petrucelli, L., Shaw, C.E., Bennett, C.F., Da Cruz, S., Ravits, J., Rigo, F., Cleveland, D.W. & Lagier-Tourenne, C. Gain of Toxicity from ALS/FTD-Linked Repeat Expansions in C9ORF72 Is Alleviated by Antisense Oligonucleotides Targeting GGGGCC-Containing RNAs. *Neuron* **90**, 535-550 (2016).

36. Livak, K.J. & Schmittgen, T.D. Analysis of relative gene expression data using real-time quantitative PCR and the 2(-Delta Delta C(T)) Method. *Methods (San Diego, Calif.)* **25**, 402-408 (2001).

37. Dastidar, S.G., Bardai, F.H., Ma, C., Price, V., Rawat, V., Verma, P., Narayanan, V. & D'Mello, S.R. Isoform-specific toxicity of Mecp2 in postmitotic neurons: suppression of neurotoxicity by FoxG1. *J Neurosci* **32**, 2846-2855 (2012).

38. Dastidar, S.G., Landrieu, P.M. & D'Mello, S.R. FoxG1 promotes the survival of postmitotic neurons. *J Neurosci* **31**, 402-413 (2011).

39. Freibaum, B.D., Chitta, R.K., High, A.A. & Taylor, J.P. Global analysis of TDP-43 interacting proteins reveals strong association with RNA splicing and translation machinery. *Journal of proteome research* **9**, 1104-1120 (2010).